Transmission System Reliability: Monitoring and Analysis

by

Meghna Barkakati

A Thesis Presented in Partial Fulfillment
of the Requirements for the Degree
Master of Science

Approved July 2018 by the
Graduate Supervisory Committee:

Anamitra Pal, Chair
Keith E. Holbert
Yang Weng

ARIZONA STATE UNIVERSITY

August 2018

ABSTRACT

Alternative sources of power generation interconnected at the transmission level have witnessed an increase in investment in the last few years. On the other hand, when the power systems are being operated close to their limits, power system operators and engineers face the challenge of ensuring a safe and reliable supply of electricity. In such a scenario, the reliability of the transmission system is crucial as it ensures secure transfer of uninterrupted power from the generating sources to the load centers. This thesis is aimed at ensuring the reliability of the transmission system from two perspectives. First, this work monitors power system disturbances such as unintentional islanding to ensure prompt detection and implementation of restorative actions and thus, minimizes the extent of damage. Secondly, it investigates power system disturbances such as transmission line outages through reliability evaluation and outage analysis in order to prevent reoccurrence of similar failures.

In this thesis, a passive Wide Area Measurement System (WAMS) based islanding detection scheme called Cumulative Sum of Change in Voltage Phase Angle Difference (CUSPAD) is proposed and tested on a modified 18 bus test system and a modified IEEE 118 bus system with various wind energy penetration levels. Comparative analysis between accuracies of the proposed approach and the conventional relative angle difference approach in presence of measurement errors indicate a superior performance of the former. Results obtained from the proposed approach also reveal that power system disturbances such as unintentional island formations are accurately detected in wind integrated transmission systems.

Quantitative evaluation of the transmission system reliability aids in the assessment of the existing system performance. Further, post-mortem analysis of failures

is an important step in minimizing recurrent failures. Reliability evaluation and outage analysis of transmission line outages carried out in this thesis have revealed chronological trends in the system performance. A new index called Outage Impact Index (OII) is also been proposed which can identify and prioritize outages based on their severity. This would serve as a baselining index for assessing and monitoring future transmission system performances and will facilitate implementation of reliability improvement measures if found necessary.

Dedicated to

my loving and supportive parents,

Ma & *Deta*

ACKNOWLEDGMENTS

I take this opportunity to express my sincere gratitude towards my advisor, Dr. Anamitra Pal who has supported and guided me throughout the course of this research work. I had always dreamt of writing a thesis as a part of my Master's degree and I am thankful to him for giving me an opportunity to work under his supervision.

I would like to thank my committee members Dr. Keith E. Holbert and Dr. Yang Weng for taking their time out to be on my thesis committee and for their valuable inputs. I would also like to thank Dr. John M. Undrill for his guidance and insights during my interactions with him.

And finally, I would like to express my deepest gratitude towards my family members for their relentless support and encouragement. I am also thankful to my friends and anyone who has directly or indirectly extended their help in completion of this thesis.

TABLE OF CONTENTS

Page

CHAPTER Page

LIST OF TABLES

LIST OF FIGURES

CHAPTER 1

INTRODUCTION

Electricity is one of the most widely used forms of energy today and our socio-economic needs are largely dependent on a reliable power supply. As a nation progresses, power systems are made to operate close to their maximum capacities to meet the increasing energy demand [1]. Environmental concerns and clean energy regulations have promoted large-scale investments in alternative energy sources and consequently, both conventional and renewable generation must meet the growing electricity demand together. These changes exert stress on the existing power system infrastructure making it vulnerable to disturbances such as faults and failures [2]. While failure is inevitable in any engineering system, the occurrence and recurrence of failures can be minimized in a power system through system reliability monitoring, performance evaluation, and outage analysis [2]-[5].

Monitoring of Transmission System Reliability:

When a disturbance occurs, it is crucial to identify the cause of the disturbance and take prompt corrective action for system restoration. Protective relaying schemes are designed to detect abnormal operating parameters and isolate faulty sections, thereby helping a power system to regain a stable operating state [6], [7]. In addition to the protection system, situational awareness is credited to reduce the extent of damage caused by power system disruptions through early detection of anomalous system behavior and facilitating prompt operator decisions [4]. The North American Electric Reliability Corporation (NERC) reported insufficient situational awareness of conditions and contingencies as one of the major causes of the August 2003 Northeast Blackout and the September 2011 Southwest Outage. The importance of monitoring bus voltage phase angle difference as a system stress and stability indicator is also emphasized in [4]. Phasor

Measurement Units (PMUs) provide synchronized measurements of voltage and current magnitude and phase angle across various buses in a power system. The Wide Area Measurement System (WAMS) utilizes these measurements to monitor the performance and provide insights into dynamic behavior of the power system in real time [8].

Analysis of Transmission System Reliability:

Power system operators continuously thrive to ensure that reliability of power supply is maintained and the energy demand is met securely and consistently. A transmission line trip may result in overloading of the alternate paths which may in turn lead to a series of line trips. During severe contingencies, this may cause an outage or in an extreme situation, a blackout [6], [8]. To prevent the occurrence and recurrence of failures, it is important to measure the performance of the existing system, assess the extent of damage caused by the incident, and identify significant contributors. Reliability evaluation and postmortem outage analysis assist in evaluating existing system's performance, revealing weak areas, identifying and prioritizing system risks [3], [5]. Based on a detailed outage analysis, operational practices and maintenance strategies can be developed for improving the system performance.

1.1. WAMS-based Islanding Detection Scheme for a Wind Integrated Bulk Power System

Uncontrolled power system islanding is a result of severe disturbance and signifies an electrical isolation of a portion of the electrical network from the remainder of the system [8]. During an island formation, the isolated region may continue to cater to the local demand in presence of adequate generation. However, during this separation, both the grid and the islanded region lose observability of each other. Before the system can be restored, it should be ensured that the islanded system survives the incident by maintaining a relative balance between load and generation [9].

The role of PMUs in detecting, identifying and maintaining an island formation during the 2008 Hurricane Gustav has been emphasized in [9]-[12]. Frequency measurements from PMUs obtained during the island formation helped operators monitor the island's load generation balance by adjusting governor controls which prevented eventual system collapse. Tokyo Electric Power Company, Inc. (TEPCO) has acknowledged phase angle difference obtained from PMUs as one of the best suited methods for detecting island formation in [13]. However, PMU measurements are susceptible to PMU and instrumentation channel errors in presence of which, accuracy of the islanding detection schemes may be affected [14], [15]. In addition, renewable energy penetration in the transmission network is expected to increase the contribution of converter fed generation such as wind and solar at the transmission level. During transients, a high renewable energy penetration may have significant impact on system stability and operations [16]. Therefore, the impact of renewable energy penetration at the transmission level and errors in PMU measurements on the performance of islanding detection scheme must be analyzed.

1.2 Reliability Evaluation and Outage Analysis of the Bulk Transmission System

Reliability of the transmission system ensures secure transfer of uninterrupted power from the generating sources to the load centers and is thus of utmost importance to both utilities and consumers. Evaluation of reliability is a crucial component during the planning, design, operation, and maintenance phases of the power system [3]. Furthermore, detailed analysis of system reliability may reveal vulnerable areas in the transmission network and establish a chronological system performance that would serve as a guideline for future reliability assessment. Transmission line outage is a power system disturbance which may occur due to various causes ranging from environmental factors such as hurricanes or blizzards to electrical equipment failures. Equipment failure may

occur due to component aging or hidden failures that aggravate during system stress [17]. An outage in the transmission network is detrimental as it can lead to a reduction in transfer path redundancy and/or capacity. Furthermore, the outage duration, which indicates the time for which the line is unavailable, may vary, ranging from less than a minute to several hours [18]. The extent of economic loss and equipment damage due to an outage can be reduced by evaluation of the existing system reliability and post mortem analysis of line outages. Outage analysis provides insight into system performance, minimizes chances of recurrence through preventive actions such as tree trimming, and reduces outage duration intensity through deployment of an emergency team during storms. The contribution of transmission system reliability evaluation and outage analysis in preventing outages and reducing the extent of damage is a substantial area of research.

1.3. Overview of the Thesis

This thesis is organized as described below:

Chapter 1 is an introductory chapter which outlines the topics covered in the thesis. This chapter highlights the importance of power system reliability and how monitoring and analysis of the bulk transmission system improves the performance of the power system. Chapter 2 focuses on detecting and identifying power system disturbances during extreme conditions such as hurricanes or floods leading to islanding. Chapter 2 provides an overview of the existing literature, ongoing research and identify gaps in existing literature for islanding detection schemes. In chapter 2, a new passive islanding technique is also presented and tested. Results obtained from simulations are compared with existing techniques in the presence of different types of errors. Chapter 3 highlights the scope and importance of transmission reliability metrics and how post mortem outage analysis helps in assessing and comparing the performance of the transmission lines. The results in Chapter 3 focus on analyzing failures such that power system operators can prevent

occurrence of similar outages due to any operational practices, planning engineers can plan augmentation of lines in case overloads are frequent, and maintenance engineers can improve maintenance strategies. Chapter 3 emphasizes on the importance of reliability evaluation and analysis and their role in improving power system performance. Chapter 4 concludes the thesis and discusses the scope of future work found relevant during the course of carrying out this work.

CHAPTER 2[1]

WAMS-BASED ISLANDING DETECTION SCHEME FOR A WIND INTEGRATED BULK POWER SYSTEM

Power system islanding is a result of severe contingencies and research in the field of islanding detection is of great interest. However, majority of the research work concern islanding detection at the distribution level. In this chapter, a passive islanding detection technique is proposed which uses PMU measurements to detect islands in a wind integrated bulk power system and is also immune to PMU measurement errors.

2.1. Theoretical Background

2.1.1. Power System Islanding

During a normal power system operation, the power balance equation is given by

$$P_g - P_e = \Delta P \qquad (2.1)$$

where, P_g is the total generation, P_e is the electrical load and ΔP is the active power mismatch.

During a power system islanding, a portion of the power system is electrically and geographically isolated from the rest of the grid. During such scenarios, each generator in the islanded power system compensates for the power mismatch with the help of the synchronizing power coefficient, K_i [19]. The behavior of the machine during this condition can be given by

$$\frac{2dH_i\omega_i}{\omega_s dt} = K_i \Delta P \qquad (2.2)$$

where, H_i is the inertia constant of the unit in s and ω_i is the rotor speed in rad/s

[1] This chapter is based on publishable work

Contribution of all the network generators in response to the disturbance is given by [19]:

$$\frac{2}{\omega_s}\sum_{i=1}^{n}\frac{dH_i\omega_i}{dt} = \sum_{i=1}^{n} K_i\Delta P = \Delta P \qquad (2.3)$$

The weighted average of rotation speed and its rate of change is given by (2.4) and (2.5), respectively[19]

$$\bar{\omega} = \frac{\sum_{i=1}^{n} H_i\omega_i}{\sum_{n=1}^{i} H_i} \qquad (2.4)$$

$$\frac{d\bar{\omega}}{dt} = \frac{\sum_{i=1}^{n}\frac{dH_i\omega_i}{dt}}{\sum_{i=1}^{n} H_i} \qquad (2.5)$$

Substituting $\omega = 2\pi f$ in (2.5) and using it in (2.3), we obtain

$$\frac{d\bar{f}}{dt} = \frac{f_s\Delta P}{2H} \qquad (2.6)$$

When an island separates from the grid, the total inertia constant of the island would be lower in comparison to that of the rest of the grid. For an active power imbalance ΔP, the rate of change of frequency of the islanded system would dynamically increase while the remainder of the grid would be in contrast more resistant due to a higher equivalent inertia constant [19]. As the resulting frequency deviates from its nominal value, a frequency difference is created which leads to the phase angle to increase with time. The increase however is dependent on several factors such as generator inertia and power imbalance [20]. In [21], the effectiveness of using change in angle over the change in frequency in detecting island formation with small power imbalances is discussed. The relationship between change in angle and frequency change is given by

$$\Delta\theta(t) = \Delta f(t)\times t \qquad (2.7)$$

2.1.2. Bus Voltage Phase Angle Measurement

Active power flows from a higher to lower voltage phase angle in an electrical network [22]. The voltage phase angle governs the active power transfer P_{xy} across a

transmission line connecting buses X and Y and vice versa as depicted in Figure 2.1. P_{xy} can be approximated [4] by

$$P_{xy} = \frac{V_x V_y}{X_{xy}} \sin(\theta_x - \theta_y) \qquad (2.8)$$

Figure 2.1: Transmission line interconnection for bus X and Y

where, $\theta_x - \theta_y$ is the phase angle difference between the bus voltages V_x and V_y. The bus voltage magnitudes V_x and V_y are maintained at a constant value near 1 p.u during normal operations. The phase angle is thus dependent on the power flow P_{xy} and reactance X_{xy} of the line. Large phase angles indicate greater power flow between two points and can lead to system instability and loss of generator synchronism [4], [22]. Phase angles may also change based on topology of the system even if the power flow between two points do not change [4]. From [22], it can be assumed that a pure sinusoidal signal can be represented by (2.9) and its phasor representation is given by (2.10). A signal is represented in a sinusoidal and phasor form by Figure 2.2.

$$v_1(t) = V_m \cos(\omega t + \phi) \qquad (2.9)$$

$$V_! = \frac{V_m}{\sqrt{2}} (\cos\phi + j \sin\phi) \qquad (2.10)$$

In (2.9), the magnitude of the phasor is given by the RMS value $\frac{V_m}{\sqrt{2}}$, ω is the frequency and the phase angle ϕ is arbitrary as it depends upon the choice of the reference t = 0.

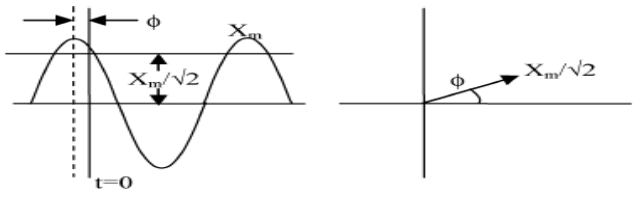

Figure 2.2: Phasor representation of a sinusoidal waveform [23]

Now, a second sinusoidal voltage signal with the same frequency ω and the same peak amplitude V_m , but with a different phase angle δ can be considered. This signal is represented by

$$v_2(t) = V_m \cos(\omega t + \delta) \qquad (2.11)$$

The phase angle difference between the two sinusoidal voltages at the same time reference can be given by

$$\text{Angle Difference} = (\phi - \delta) \qquad (2.12)$$

Two voltages from different locations can be represented by equations (2.9) and (2.11) and if they are time tagged, then the relative phase difference of one voltage can be calculated with respect to the other by (2.12) [22]. In a similar way, relative phase angle difference of other voltages that are also time tagged but obtained from different locations can be calculated using the same reference signal.

2.1.3. Role of PMUs in Phase Angle Monitoring

Phasor Measurement Units (PMUs) were invented in early 1980s and with the implementation of Wide Area Measurement System (WAMS), PMUs have been increasingly used worldwide for applications such as power system monitoring, protection and control [23]-[32]. PMUs provide time synchronized current and voltage phasors (magnitude and phase angle) as well as frequency measurements at a rate of 30-60 samples per second, and are significantly faster than their Supervisory Control and Data Acquisition (SCADA) counterparts [22]. PMUs can therefore provide power system operators an overview of the system dynamics in real time.

A common technique for PMUs to determine phasor representation of an input signal is to apply a Discrete Fourier Transform (DFT) to data samples of the signal. The phasor representation of N data samples taken over one period is given by [23].

$$V = \frac{\sqrt{2}}{N} \sum_{i=0}^{N-1} v_i \varepsilon^{-ji\frac{2\pi}{N}} \qquad (2.13)$$

PMUs have witnessed a wide deployment after the 2003 and 2011 North American power disturbances. Per the North American Synchro Phasor Initiative (NAPSI), over 1700 production grade PMUs have been installed across North America as of 2014 [33]. Figure 2.3 is a pictorial representation of the PMUs installed in the North American Power Grid as of March 2015.

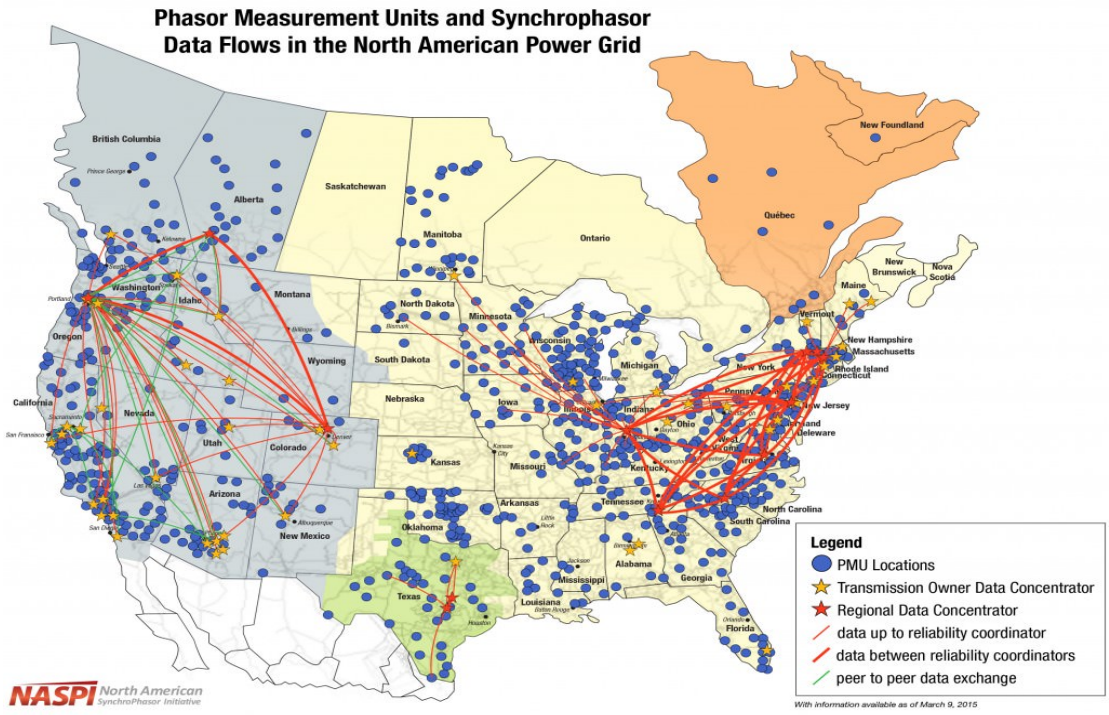

Figure 2.3: PMU locations across North American Power Grid [33]

As PMUs monitor the grid continuously and provide time synchronized measurements, voltage phase angles obtained from PMUs can be used to calculate relative phase angle differences across a network [22]. PMU based angle monitoring is used by electric utilities and grid operators for a number of applications such as wide-area situational awareness and visualization, setting alarms, alerts and improving state estimator solutions[14], [22]. Significant change in phase angle difference across an

interconnection indicates increase in system stress and may be regarded as a precursor to a power system disturbance [4], [22].

It is acknowledged that development of a reliable and fast islanding detection technique without nuisance tripping and non-detection zones is an ongoing challenge [34]-[36]. In the literature, most techniques for unintentional islanding detection or anti islanding protection are being developed specific to distributed energy resources (DER) [36]-[51]. However, wind energy contribution in the bulk power system is expected to increase in the future, with more utilities investing in wind power generation interconnected at the transmission level[1]. As is evident from Figure 2.4, wind energy is the fastest growing renewable source of energy in the United States over the last 10 years and constitutes approximately 6% of the total electricity generation [52]. From Figure 2.5, wind energy contribution is observed to be around 25% of the total electricity generation in as many as 5 states as of 2017.

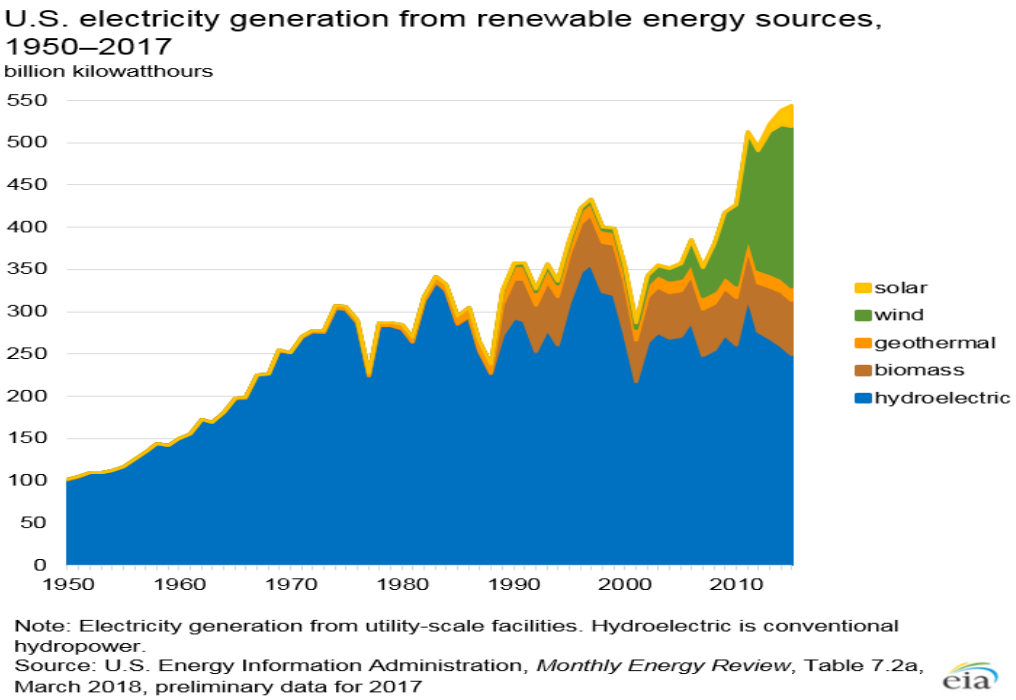

Figure 2.4: US electricity generation from renewable energy sources (1950-2017) [52]

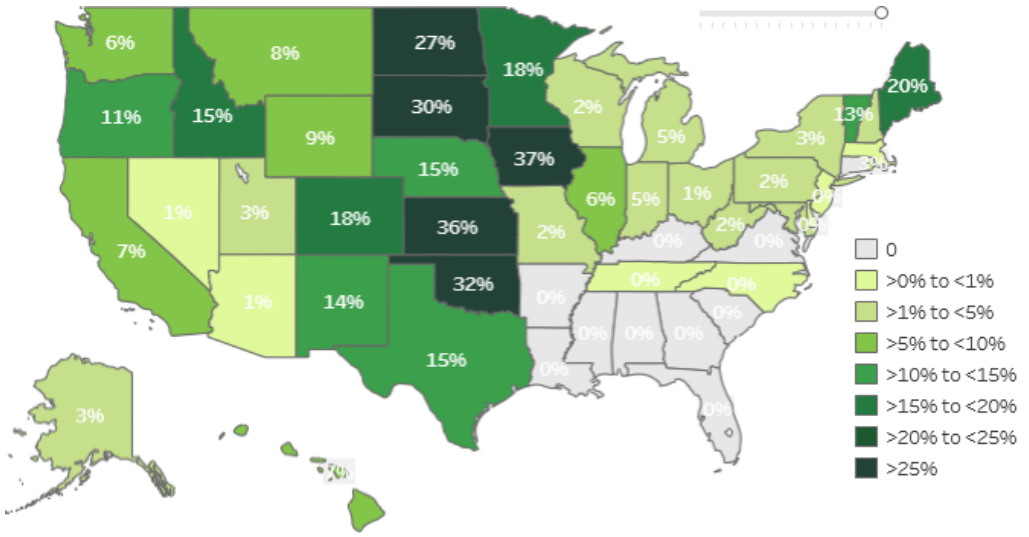

Figure 2.5: Wind Energy's Share of State Electricity Generation [53]

Investigation of large scale wind and solar energy integration in power system dynamic response is an area that attracts attention in the research world. This was examined in a study carried out by the National Renewable Energy Laboratory (NREL) in 2014, where it was observed that although transient stability of the WECC system did not change fundamentally with high wind and solar penetration, it did not indicate that the system behaved identically as in the absence of renewables [54]. Likewise, during island formation, the transmission system would be subjected to dynamics and its response with high renewable penetration would be an interesting subject of analysis.

2.1.4. Motivation and Objectives

Based on discussions with Commonwealth Edison (ComEd) during the course of this work, wind power utilities typically prefer to trip an islanded wind farm using frequency and voltage based protection schemes. However, due to change in system topology during uncontrolled islanding or even protection relay failures, there could be an instance when predetermined protection schemes fail to detect a wind farm's isolation from the grid [34]. Electrical network augmentations are not uncommon in the grid and it might be possible that a portion of the network is not modeled in the SCADA system [19].

In such cases, the status of all breakers in the network may not be available for monitoring. Considering the aforementioned scenarios, it is conceivable that existing islanding detection techniques may fail.

This research work aims to address the following objectives:

1) Performance in a wind integrated transmission system: As the ongoing research work primarily focuses on detection methods associated with DER [36]-[51] , the performance of an islanding scheme in detecting and identifying islands in a wind integrated bulk transmission system must be examined.

2) Performance in presence of PMU errors: PMU measurements are no exception to measurement errors which cause deviations in any measured quantity. In the case of PMU based islanding schemes, it has been observed that instrument errors may affect the accuracy of island detection [15]. The accuracy of the proposed technique in presence of PMU measurement errors therefore must be examined.

2.2. Literature Review of Islanding Detection Schemes

Ongoing research in the field of islanding classifies islanding as [9]:

- Controlled islanding: Often employed as a part of protection scheme where multiple islands are intentionally created during severe power system stress to prevent entire system collapse. Load-generation imbalances are maintained at a minimum within these islands.
- Uncontrolled islanding: These are spontaneous and occur against a utility's planning and are classified as power system disturbances. Uncontrolled islands can be formed due to numerous reasons such as multiple line trips on account of natural calamities or electrical equipment malfunctions due to hidden failures.

Uncontrolled islanding can create large or small islands. The 2008 Hurricane Gustav rendered several transmission lines out of service and created an island which had

a load of around 3000 MW. This was a large island that was successfully maintained by adjusting governor controls using frequency information obtained from PMUs installed outside and inside the island for over a day [9]-[12]. Smaller islands are typically formed with loads not greater than 100 MW and the island can be maintained by internal generation and load shedding. Islanding duration can last from a few minutes to hours and sometimes even days. It is therefore necessary to detect islands as soon as they are formed so that remedial action can be taken initially for its survival, and eventually for its reconnection with the grid. Detection techniques in the literature fall into three categories [36]:

- Active methods: Involves injection of disturbance into the network and islands are detected on the basis of system response to these disturbances. These methods are however intrusive in nature and may degrade the power quality of the supply [38], [39].
- Passive methods: Involves analysis of system behavior based on direct or derived operating parameters such as voltage, frequency or power. These are non-intrusive in nature and therefore, preferred. Some examples of passive detection techniques are listed below:
    - Protection schemes based on frequency or voltage measurements [39],[40]
    - FNET based on FDR measurements [8], [51]
    - WAMS based on PMU measurements [9], [41]
- Communication based: Remote detection techniques do not have Non Detection Zone in theory and are very reliable. These involve communication of circuit breaker status to trip DGs when islands are formed but installation of a communication based detection system can be expensive[36],[55].

2.2.1. Existing Passive Islanding Detection Techniques

In view of the drawbacks of the existing active and communication based islanding detection schemes highlighted above, this thesis focuses on passive islanding detection schemes. These can be further described as below:

Protection relaying schemes:

Wind farm anti islanding protection schemes typically use frequency and voltage parameters to detect island formation and trip the wind farms once they are separated from the grid. Anti-islanding protection schemes are implemented through numerical relays and operate on derived quantities such as rate of change of frequency (ROCOF) or voltage vector shift (VVS) [20],[40].

WAMS based schemes:

According to a report submitted by NASPI in 2016 [22], PMU based angle monitoring tools are being used by utilities and grid operators in the United States for calculating and setting phase angle difference alarms. This is done with an aim to provide real time grid situational awareness and indicate system stress. The entities use commercial or in-house developed software for phase angle monitoring. Some commercial vendors include EPG – RTDMS, OSIsoft – PI historian, SEL0 SynchroWAVe Central, etc. The relative phase angle difference is calculated based on (2.12) [56]. One of the strategies employed by Entergy to maintain the island formed during the 2008 Hurricane Gustav was based on this technique [9]-[12]. WAMS based schemes can be classified further as:

FNET based: Frequency monitoring network (FNET) is a low cost wide area phasor measurement system installed in the distribution system. FNET based islanding detection has been used to detect island formation using frequency difference or change of angle difference method and has been described in [8]. Islands are detected when the frequency

difference or change of angle difference exceeds the predetermined thresholds of limits and time.

PMU based: An islanding detection scheme based on change in angle difference of the distributed generation source and the utility substation angles is proposed in [21]. An island is detected if the calculated angle difference exceeds the set threshold. Another technique by Tokyo Electric Power Company (TEPCO) uses a synchronization control scheme between different substations to calculate the angle difference between bus voltage phase angles [12]. When the calculated angle difference is larger than a preset threshold, an islanded condition is detected.

Data mining based: Principal Component Analysis (PCA) based islanding detection methods are discussed in [49], [57], however these are associated with huge computational burden. A local islanding detection technique for distributed generation using cumulative sum of change in positive sequence voltage phase angle is proposed in [50]. This approach is beneficial in detecting islands with low power mismatch and has a faster detection time. Decision tree based islanding detection techniques have been proposed in the literature that correctly predict island formation with high accuracies using real time data [9], [58].

2.2.2 Gaps in Existing Passive Islanding Detection Schemes

Protection relaying schemes:

High sensitivity of ROCOF relays have reported mal-operation during remote faults. As a solution to this problem, a higher ROCOF threshold has been opted for, however, this has led to an increase in the non-detection zones [35], [61]. These thresholds however are subject to change with changing system conditions and faster detection times are preferred during any power system disturbance [35]. As per [13] frequency based islanding schemes are not effective when the frequency difference

between the islanded portion and the rest of the grid is insignificant giving rise to the issue of non-detection zones in such scenarios [21].

PMU based: PMU based islanding detection techniques used in the literature such as the voltage phase angle difference approach depends on the selection of the reference phase angle [35]. In the single reference approach, the angle difference depends on a single reference location and signal quality. It is at times prone to large non-detection zones or mal-operations. Multiple reference approach use more than one reference signal from multiple locations around the network and is more robust. However, one disadvantage with PMU based detection techniques is the effect of PMU measurement errors. The PMU measurement errors comprise of [14]:

- PMU device errors: In a PMU, when sinusoidal input signal is converted to phasor form using DFT as represented in (2.9), the harmonics in the signals are eliminated after filtering the signal. However non-harmonics and random noise in the input signal result in an error in the phasor estimate [23].
- Instrumentation channel ratio errors: Current and voltage transformers provide stepped down levels of currents and voltages to the PMU inputs. Although instrument transformers are high accuracy class measuring instruments, the name plate rating of these transformers may vary from the actual conversion ratios. This may be due to reasons such as aging, environmental conditions and circuit burden [14].

While traditionally PMU measurement based voltage angle difference monitoring between two buses across the disconnected systems have been used for islanding detection [13], [21], [22], noise due to instrument transformers can severely degrade the measurements. Errors in the phase angles can be as high as $\pm 4^{\circ}$ [14], which can alter the efficiency of the angle difference based detection technique [15] as illustrated in the example below.

Let us assume two PMUs are placed on buses 3 and 13 in the 14-bus system shown in Figure 2.6. An islanding detection technique monitors the difference of real-time voltage angles between buses 3 and 13. Let the voltage angle measured by a PMU at Bus 3 (PMU_3) be θ_{3m} and that at Bus 13 (PMU_{13}) be θ_{13m}. Now, the measured voltage angle difference between the two buses is given by

$$\Delta\theta_m = \theta_{3m} - \theta_{13m} \tag{2.14}$$

When the calculated voltage angle difference, $\Delta\theta_m$ exceeds an offline-determined threshold τ, an island is detected. It must be pointed out here that τ is obtained from offline analysis and does not account for the actual instrumentation channel errors that are present in the system. Now, suppose the instrument transformer error in PMU_3 measurement is -3° and that in PMU_{13} measurement is +2°. Also, let τ be 80° and the true voltage angles of Bus 3 and Bus 13 with respect to a reference be 70° and -12°, respectively. Therefore, the true angle difference will be 82° (=70°-(-12°)) which is above the threshold, and indicative of an islanded system. However, due to the instrumentation transformers errors present at the two buses, $\Delta\theta_m$ would actually be 77° (=70°-3°-(-12°+2°)), which is below the threshold, and hence the island formation would not be detected. Thus, we can see how in presence of errors in a real system, a voltage angle difference based islanding detection technique may misclassify island formation.

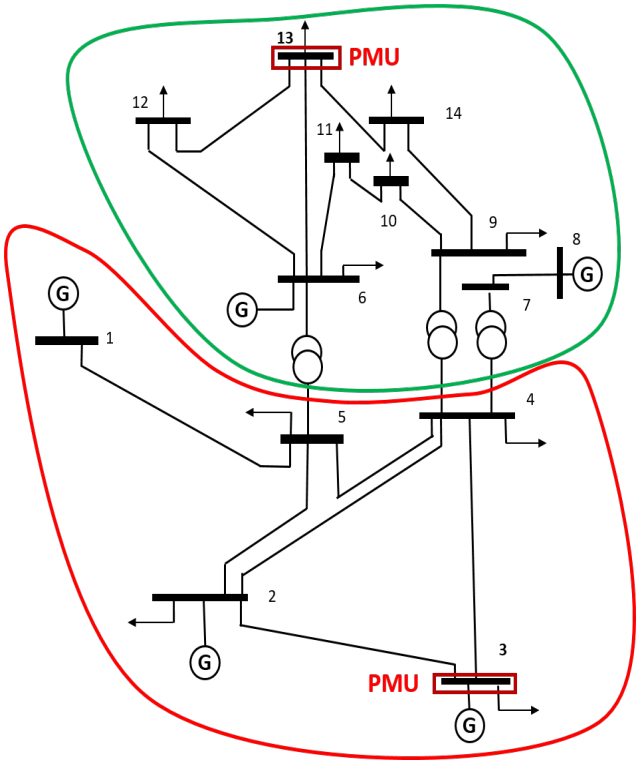

Figure 2.6: Modified 14 bus system 0

Usually ratio errors are not included in the simulation phase, and when PMU based applications are implemented in real time, in the presence of maximum phase angle measurement errors, the calculated angle measurements may vary from their true values by as high as 8◦ [14] . It can be observed how this may adversely affect the accuracy of an islanding detection scheme as discussed in the example above. Thus, it can be concluded that angle difference based islanding detection schemes would perform unsatisfactorily in the presence of PMU errors [15]. With reference to the issues highlighted above, we can understand the need to develop a robust scheme which can detect island formation in the presence of PMU errors in the bulk transmission system.

2.3. Wind Energy Integration

2.3.1. Wind Energy Basics

Wind turbines convert the kinetic energy of the wind into mechanical energy, which is subsequently converted into electrical energy through a generator. Wind power is of three key types [59]:

- Utility scale wind: The wind turbines are typically rated above 100 kW and are connected to the grid via step up transformers
- Distribution scale wind: Wind turbines lower than 100 kW in capacity and directly connected to a residence or farm.
- Offshore wind: These are installed on water bodies due to availability of higher wind speeds.

Wind turbines are mounted on tubular steel towers with a hub attached to three blades and a nacelle which encloses the shaft, gearbox, generator, and controls. [59].

2.3.2. Wind Turbine Modeling

Wind turbines are primarily of four types [63]:

- Type 1: Cage rotor induction generators
- Type 2: Induction generators with variable rotor resistance
- Type 3: Doubly fed asynchronous generators with rotor-side converter
- Type 4: Full converter based wind turbines

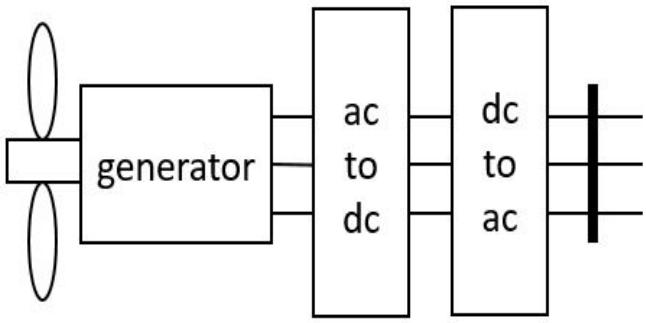

Figure 2.7: Type 4 full converter wind turbine [63]

The full converter type 4 wind turbines are the one of most frequently installed wind turbines. In these types of wind turbine models, the generator is decoupled from the rest of the electrical system through converters [59]. Figure 2.7 represents this type of a wind turbine.

An individual wind turbine is typically rated for capacities 1-4 MW at around 690 V. A wind farm is a collective group of interconnected wind turbines that are tied to a point of common coupling before the power is fed to the grid. In accordance with the WECC Wind Plant Power Flow Modeling Guide, wind plants must be represented by an equivalent generator, generator transformer, and collector system and substation transformer [64] as depicted in Figure 2.8. Several wind turbines are connected to a grid as depicted by the aggregated wind turbine at bus 5. A pad mounted generator step up transformer usually steps up the generation voltage of 600-690V to 34 kV. In the figure this is represented by the transformer between buses 5 and 4. Multiple wind turbine models are connected at the 34 kV collector bus between buses 4 and 3. The operating voltage at the collector bus is further stepped up at the interconnection to the transmission voltage level at 132 kV or 230 kV via a substation transformer as represented by transformer between buses 3 and 2. The collector system which is then interconnected to the transmission system at bus 2 via step up transformers. The representation below is

considered adequate for positive sequence dynamic simulations and thus the wind farms in this research work are modeled on the basis of it [63].

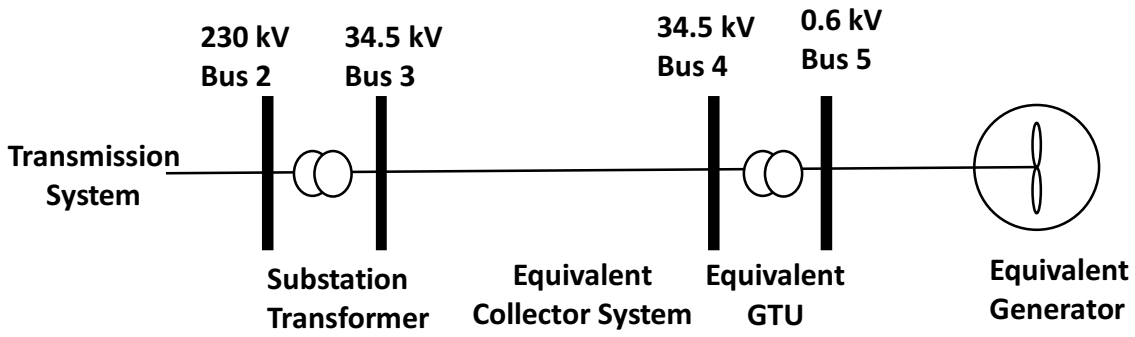

Figure 2.8: Wind turbine Single Line Diagram [64]

GE PSLF software is used to carry out dynamic simulations and type 4 wind energy generator, turbine and exciter models are used to represent the wind power penetration in the system. The PSLF models used for modeling of wind energy penetration in the research work are as follows [63]-[66]:

- Wt4g: Generator/converter model for Type-4 (Full converter) wind turbines is the interface between the generator and the rest of the electrical network.
- Wt4e : Simplified exciter model for Type-4 (Full Converter) represents the electrical control of the wind turbine.
- Wt4t: Simplified wind turbine Type-4 (Full Converter) model represents the controls and mechanical dynamics of the wind turbine.

2.4. Proposed Islanding Detection Methodology

In this research work, a WAMS based passive islanding detection technique is proposed which utilizes a data mining model to identify and detect island formation in the transmission system. This approach uses a derived voltage phase angle parameter obtained from PMU measurements - *Cumulative Sum of Change in Voltage Phase Angle Difference (CUSPAD)*. In this section, the implementation of this methodology is

described and its effectiveness in presence of wind energy penetration and PMU errors is evaluated. The results are then compared with those of the conventional angle difference technique.

2.4.1. Data Mining Model

The islanding detection algorithm in the proposed approach utilizes Decision Trees (DTs). DT is a supervised learning data mining technique which draws hidden relationships in the data and classifies data based on binary partitioning decisions through if-else statements [67]. In this technique, a Classification and Regression Tree (CART) based DT is trained offline with the help of a training database and a model is developed by finding correlations between the input and the output. In Figure 2.9, a DT structure example is presented where the parent node represents the complete dataset. At each node, the dataset is split into two subsets and the process is continued till no further splits are possible [67]. After the DT model is built, a testing dataset is processed through if-else conditions and a decision is obtained based on predetermined splits. In [9], [58], and [68] it has been observed that DT based classifiers detect island formation accurately and reliably and therefore in this research work, DTs are used to evaluate performance of the proposed methodology. Some terminologies with respect to DT are described below [69]:

- Size: The size of the DT is given by the total number of nodes present in the tree.
- Depth: DT depth is the longest path between the root and the leaf node. In Figure 2.9, the root is the parent node while the splitting nodes are the leaf nodes. In this example, the depth of the DT is 3.
- Pruning: Pruning is a process by which the size of the DT is reduced by removing sections that are less significant with regards to some pre-determined metric.

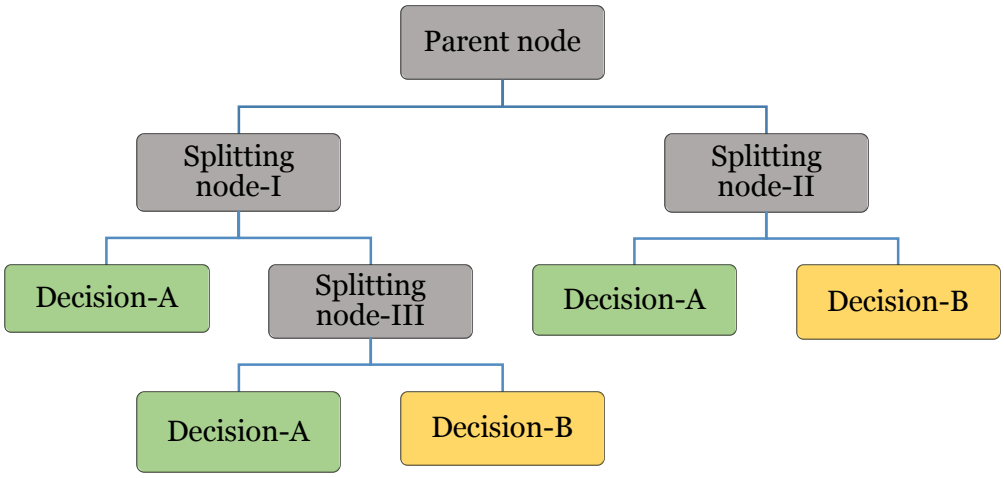

Figure 2.9: CART example

2.4.2. Input Feature

Figure. 2.10: Voltage angles across transmission line interconnecting Bus X and Y

From figure 2.10, the voltage phase angle at bus X is θ_x and that at bus Y is θ_y. The phase angle difference between bus X and Y at time instant, $t = 0$ is given by

$$\Delta\theta_{xy}^{0} = \theta_x(0) - \theta_y(0) \tag{2.15}$$

Now suppose, an island is formed at time instant, t. The phase angle difference between bus X and Y after the island is formed is given by

$$\Delta\theta_{xy}^{t} = \theta_x(t) - \theta_y(t) \tag{2.16}$$

The relative change in the angle differences between the two instants $t = 0$ and $t = t$ can be calculated by [8]:

$$\Delta\theta_{xy}^{t-0} = \Delta\theta_{xy}^{t} - \Delta\theta_{xy}^{0} = [\theta_x(t) - \theta_y(t)] - [\theta_x(0) - \theta_y(0)] \quad (2.17)$$

This can be rewritten as

$$\Delta\theta_{xy}^{t-0} = [\theta_x(t) - \theta_x(0)] - [\theta_y(t) - \theta_y(0)] \quad (2.18)$$

Now, (2.18) can be rearranged in terms of the individual buses' change in voltage phase angle as

$$\Delta\theta_{xy}^{t-0} = \Delta\theta_{x}^{t-0} - \Delta\theta_{y}^{t-0} \quad (2.19)$$

To minimize misclassifications, this change in voltage phase angle at each bus is accumulated over a certain time window, *w* [15]. The measurement window size is selected based on DT accuracies obtained for different window sizes, which is described in detail in Section 2.4.5. The *Cumulative Sum of Change in Voltage Angle, S* at bus x can be mathematically described by

$$S_x = \sum_{n=1}^{w} |\theta_x(t+n) - \theta_x(0)| \quad (2.20)$$

where, $\theta_x(0)$ is the steady state voltage phase angle and $\theta_x(t+n)$ is the voltage phase angle trajectory after an island has been formed.

Therefore, the *Cumulative Sum of Change in Phase Voltage Angle Difference, CUSPAD* between the two buses X and Y in the above example can be given by

$$CUSPAD_{xy} = S_x - S_y \quad (2.21)$$

This change in a voltage phase angle difference pairs between steady state and post islanding condition is used as the Decision Tree input for this research work.

CUSPAD is intended at monitoring the trajectory of change in voltage phase angle after a power system disturbance occurs. In this thesis, it is hypothesized that the trajectory of voltage phase angles for an island formation is not identical to any other power system disturbance and formulation of CUSPAD in (2.21) is expected to capture the same.

2.4.3. Database Creation and Implementation

To create the database, both islanding and non-islanding scenarios have been simulated using GE PSLF software in the following steps:

1. Generation of simulation cases: For non-islanding scenarios, some extreme cases such as line trips, faults and generator trips have been simulated, and the measurement of phase voltage angle for these cases have been recorded. For islanding cases, islands have been created by removing $i, 1 \leq i \leq 5$ transmission lines each at different instants of time.
2. Measurement of voltage phase angle: For each case simulated, the voltage phase angle measurements required for calculating CUSPAD values are obtained using the GE PSLF software model *ametr*. This model measures voltage phase angles with respect to a reference bus phase angle. It is assumed that PMUs are installed on multiple locations in the system under study and the bus voltage angle measurements are provided by them. Based on the PMU placement formulation discussed in Section 2.4.4, the locations of buses where the PMUs are to be placed to ensure system observability along with monitoring critical buses' voltage angles are determined.
3. Calculation of CUSPAD: It is assumed that a disturbance occurs at time instant t where each instant is equivalent to a PMU reporting rate of 30 samples/second. For CUSPAD calculations in the simulations carried out, the subsequent PMU voltage phase angle measurement at the $t + 1$ time instant is considered as the first sample in the measurement window. Let us assume the measurement window to be w, now the trajectory of voltage angle measurement after the disturbance is monitored till the $(t + w)^{\text{th}}$ sample. CUSPAD is then calculated from (2.21) using

the corresponding phase angle values during the steady state. In the simulations carried out, a flat run is considered as the steady state value of voltage phase angle.

4. Training Database: After the CUSPAD values for each simulation are obtained, they are fed as the input to CART based DT in MATLAB. Each of these cases are identified as an island or non-island case by labeling them as 0 or 1 [9] before feeding the data to the DT. This data serves as the training database on the basis of which the DT model is built.
5. Testing Database: Now to test the DT model built in the previous step, realistic measurements are replicated through introduction of measurement errors in the training database of true voltage phase angles. The error model used is additive and includes both PMU and instrumentation channel errors in the range:
    a. PMU errors in voltage phase angles are assumed to be a Gaussian distribution with zero mean and standard deviation of 0.104◦ [14].
    b. Instrumentation channel errors in voltage phase angle are typically assumed to be in the range of ± 4◦, ±2◦ and ± 1◦. Good quality measurements are also considered for testing purpose and assumed to have a uniform distribution zero mean and standard deviation of 0.1◦ [14].

    The resultant voltage phase angles after incorporation of additive PMU and instrumentation errors [70], [71] can be given by (2.22)

$$\theta_{actual}^{V} = \theta_{true}^{V} + \alpha_{error}^{VT} + \alpha_{error}^{PMU} \qquad (2.22)$$

    where θ_{actual}^{V} is the resultant voltage phase angle after incorporation of errors in the true voltage phase angle measurements θ_{true}^{V}. The instrumentation channel errors are denoted by α_{error}^{VT} while the PMU errors are denoted by α_{error}^{PMU}.

After errors are introduced into the training dataset, CUSPAD is recalculated using the test data and the steady state voltage phase angles. These data serve as input to test

the accuracy of the DT model. The overall model of the proposed methodology is illustrated in Figure 2.11.

While the DT model described above has been trained and tested offline, for real time implementation of the proposed technique, a pre-processing step is required before data can be fed to the DT algorithm. This is done to determine the steady state voltage angle which can be updated in real time using an auto-regressive (AR) model from [72]. In [72], it is found that the complex voltage at a future time instant can be determined from its three previous estimates as shown in (2.23). Using PMU measurements, the complex voltage at instant can be predicted using previous samples and the voltage angle θ_p can be calculated from the complex voltage.

$$\widehat{\mathrm{V}}(\mathrm{k}+1|\mathrm{k}) = 3\widehat{\mathrm{V}}(\mathrm{k}|\mathrm{k}) - 3\widehat{\mathrm{V}}(\mathrm{k}-1|\mathrm{k}-1) + \widehat{\mathrm{V}}(\mathrm{k}-2|\mathrm{k}-2) \qquad (2.23)$$

Using the predicted voltage angle (θ_p) from (2.22) and the measured voltage angle (θ_m) from the PMU measurements, an observation residual R can be calculated, which is given by

$$Observation\ Residual\ (R) = \theta_m - \theta_p \qquad (2.24)$$

When the observation residual R is greater than some threshold, CUSPAD can be calculated using (2.21).

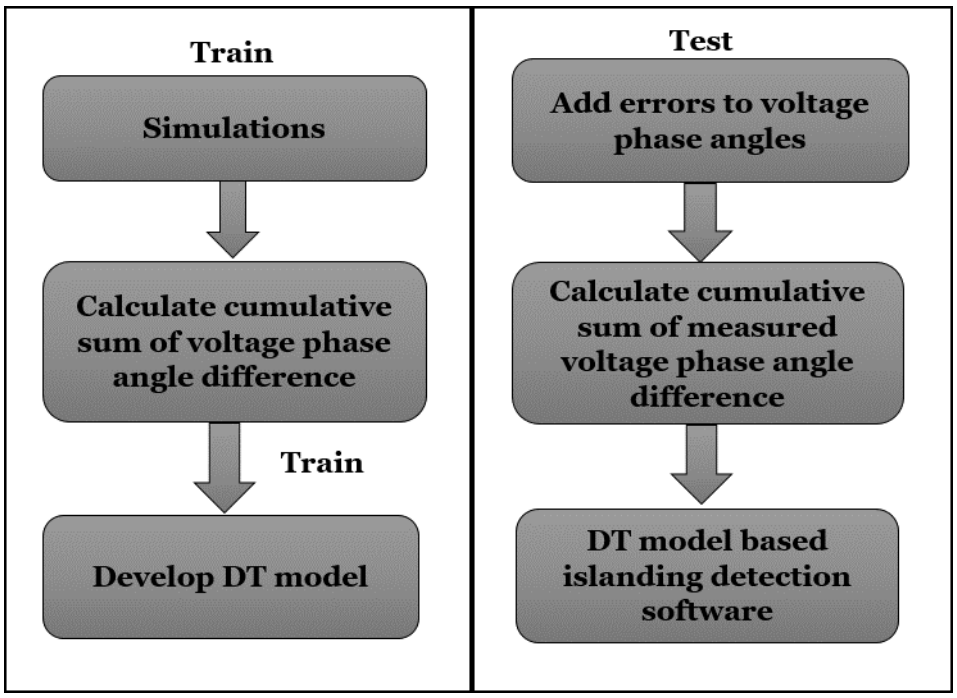

Figure 2.11: Flowchart for the proposed CUSPAD approach

2.4.4. PMU Placement

When PMUs are placed in a network, the primary objective is to ensure observability, i.e. the PMUs should have the ability to directly or indirectly measure the states of the network. In addition to ensuring topological observability, the PMU placement scheme proposed in [73] takes into consideration PMU redundancy for critical buses and substation disruption minimization. In terms of graph theory, the buses in an electrical network can be denoted as nodes $v \in V$, which are placed in a substation S which are connected by edges $e \in E$ that are either transmission lines or transformers. Dual Use Line Relays (DULRs) are digital relays that pose as PMUs by measuring voltages at one end of an edge. The optimal PMU placement formulation discussed in [74] considering the above constraints can be defined by the equations (2.25)-(2.28):

$$x_i = \begin{cases} 1, & if\ Substation\ S_i is\ distrupted \\ 0, & otherwise \end{cases} \quad (2.25)$$

For each edge, e, there are two variables

$$w_e^l = \begin{cases} 1, & if\ DULR\ is\ placed\ at\ the\ low\ end\ of\ edge\ e \\ 0, & otherwise \end{cases} \quad (2.26)$$

$$w_e^h = \begin{cases} 1, & if\ DULR\ is\ placed\ at\ \square he\ high\ end\ of\ edge\ e \\ 0, & otherwise \end{cases} \quad (2.27)$$

$$Minimize\ \left(\sum_{i=1}^{k} c_i x_i + \Delta \sum_{e \in E} \{w_e^h + w_e^l\}\right) \quad (2.28)$$

This formulation was used to calculate the locations of the PMUs in the test systems.

2.4.5. Simulation and Results for modified 18 bus case

To verify the performance of the proposed technique, the 18 bus system available in the GE PSLF library is used as a test system for carrying out dynamic simulations and generation of the database. For carrying out the simulations offline, the steady state voltage angle in (2.15) is assumed to be the angle prior to a disturbance or contingency.

Case 1: 18 Bus Test Case:

The original 18 bus system available in the PSLF library is modified to include wind energy penetration in the network by replacing one of the conventional generator at Bus 231 with an equivalent capacity aggregated wind farm connected to the 230 kV network. This system is comprised of 19 buses, 4 generators, 17 transmission lines and 7 transformers. The real power generation of the system and electrical load is approximately 3077 MW and 3000 MW, respectively.

Database:

To build the database for the islanding detection algorithm several non-islanding scenarios were analyzed such as faults, line trips, generator trips, transformer trips and generation load mismatch. The scenarios considered are summarized in Table 2.1.

Table 2.1 Summary of simulated cases

Total Cases	Islanding	Non-Islanding
467	200	267

PMU locations:

The total number of PMUs required for complete observability of this system was found in accordance with the formulation described in Section 2.4.4. The PMUs were located on buses 1, 11, 14, 23, and 31.

Window size:

To determine a suitable window length for calculating *CUSPAD*, the DT accuracies obtained with window size of 5, 10, 20, 30 and 40 samples are presented in Figure 2.12. It is observed that as the window size increases, the accuracy of DT is higher. A larger window size will influence the detection time. However as with any islanding detection algorithm, a lower detection time is preferred and therefore a compromise between DT accuracy and window size must be made. We observe that the relative increase in DT accuracy corresponding to the window size between 30 and 40 samples is less as compared to that obtained for window sizes between 20 and 30 samples.

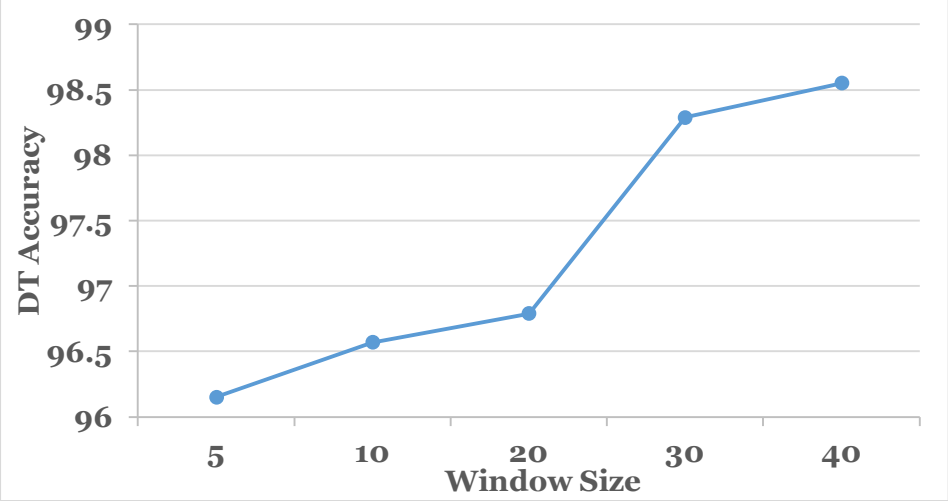

Figure 2.12: Variation of DT accuracies for CUSPAD approach with window sizes

To bring into perspective the time delays associated with islanding detection time in the literature, a time delay of 100-150 ms (corresponding to 5 samples) was considered

in [15] to prevent misclassifications during load generation imbalances. Further [35] indicates that typically 500 ms time delay (corresponding to 16 samples) is considered sufficient to prevent false detection during generator trips. Islanding detection time as high as 2-3 seconds is discussed in [8]. From the above, we can conclude that a window size of 30 samples would be suitable for simulation and analysis of the proposed approach.

Results

Voltage angle trends: For preliminary investigation, the voltage phase angle variation observed for the 18 bus system during islanding and non-islanding scenarios are plotted below.

a. Non-islanding case (three-phase fault): A three-phase fault is simulated in a selected transmission line and the voltage phase angle measured by PMUs located on Bus 1 and 14 are plotted. From Figure 2.13, it is observed that at the instant of the fault, at t = 5 seconds, the Bus 1 voltage phase angle oscillates, however it settles to a steady value soon after the fault is cleared. In this case, the phase angle difference between Bus 1 and Bus 14 does not deviate significantly from the pre-fault voltage phase angle difference.

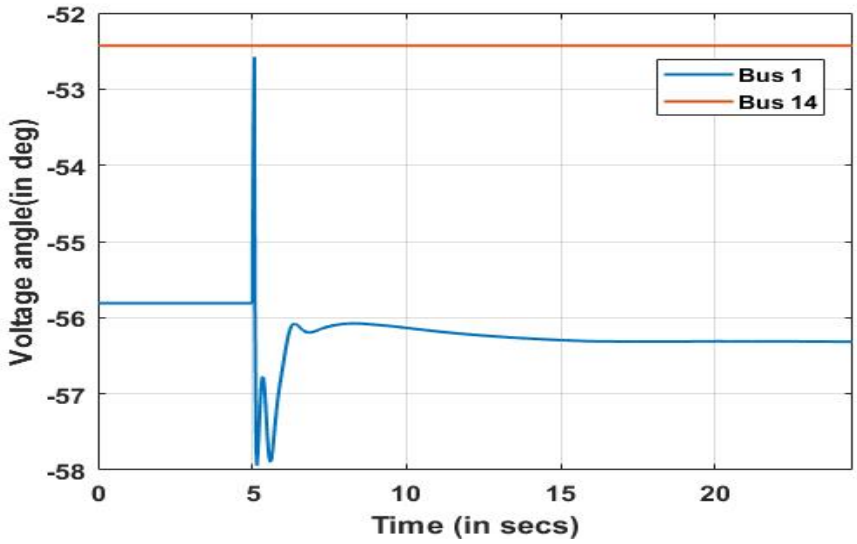

Figure 2.13: Variation of Bus 1 voltage phase angle during a three-phase fault

b. Non-islanding case (N-1-1 contingency): A N-1-1 contingency is simulated at $t = 5$ and at $t = 10$ and the voltage phase angle measured by a PMU located on Bus 1 is plotted in Figure 2.14, it is observed that at the instant at $t = 10$ seconds, the Bus 1 voltage phase angle starts to decline, however it settles to a steady value within a few seconds after the contingency. Unlike Case b, the final phase angle difference between Bus 1 and Bus 14 changes post-contingency. However, this change does not continue to increase throughout the simulation period.

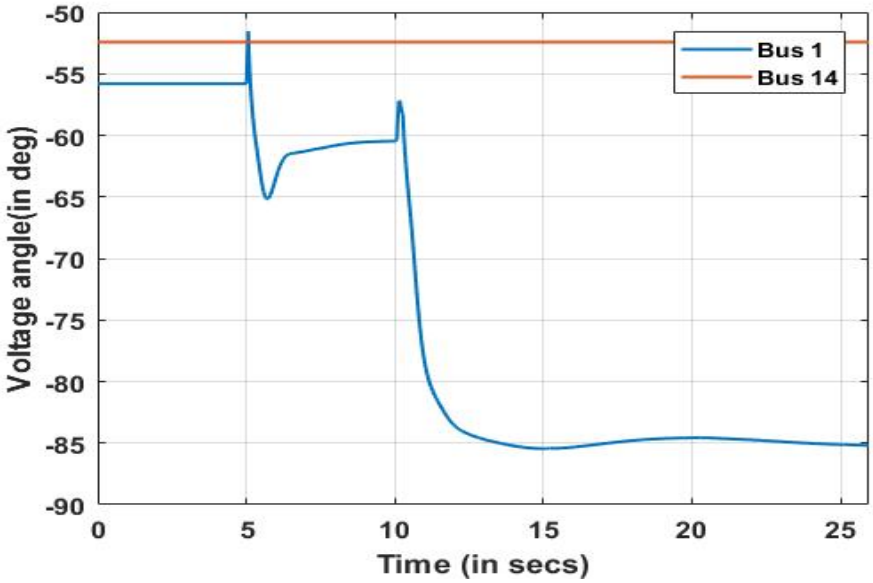

Figure 2.14: Variation of Bus 1 voltage phase angle during a N-1-1 contingency

c. Islanding case (N-1-1-1 contingency): An N-1-1-1 contingency was simulated at $t = 5$, 10 and 15 seconds resulting in an island formation at $t = 15$ seconds. From Figure 2.15, it is observed that at the instant when the island is formed, Bus 1 voltage phase angle starts deviating with respect to Bus 14 and continues to do so throughout the simulation period. The slope of Bus 1 angle variation in this case is observed to be much higher than compared to that of Case b.

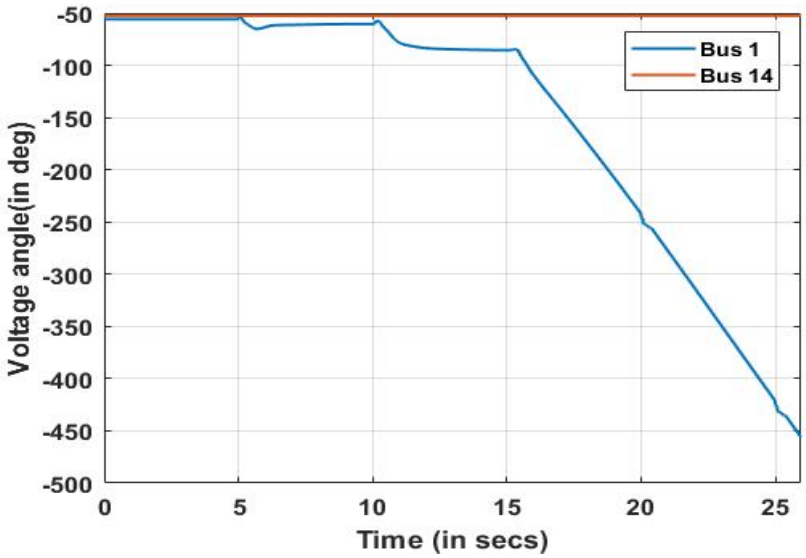

Figure 2.15: Variation of Bus 1 voltage phase angle during an island formation

Results using CUSPAD: Using the DT model obtained using a 30 sample window, the simulations were repeated 50 times and a 95% confidence interval accuracy was computed for the test data. The test data comprised of a range of measurement errors including both PMU and instrumentation channel errors. It can be observed from Table 2.2, that the testing accuracy of CUSPAD for the determined window size of 30 samples is not significantly affected by measurement errors.

Table 2.2 Summary of results for DT testing accuracies with CUSPAD approach considering measurement errors

Error		**CUSPAD**	
Systematic Error	**Random Error**	**Accuracy (95%)**	**Depth**
0	0 Mean ±0.104 SD	98.29±0.00	5
0 Mean ±0.1 SD		98.01±0.07	5
±1		98.06±0.07	5
±2		98.08±0.06	5
±4		97.97±0.08	5

Results using conventional angle difference: In this approach, the angle difference (AD) of voltage phase angles measured by PMUs at the 30th sample after a disturbance has

occurred is calculated. This is done to compare the accuracies obtained with a window size of 30 samples for CUSPAD with AD of voltage angle at the 30^{th} sample. The angle difference, is calculated for each bus with respect to the time tagged reference voltage phase angle measured from a different location in the system.

Single reference approach [35]: It can be assumed that the reference bus voltage angle θ_1 is the voltage phase angle measurement obtained from the PMU at Bus 1. The voltage phase angles at Buses 11, 14, 23 and 31 are denoted by θ_{11}, θ_{14}, θ_{23} and θ_{31}. Now using (2.12), the relative phase angle difference for the remaining buses can be calculated to obtain four angle difference pairs $\theta_{11} - \theta_1$, $\theta_{14} - \theta_1$, $\theta_{23} - \theta_1$ and $\theta_{31} - \theta_1$. This is fed into the DT and training accuracies are obtained. Similarly, the accuracies of relative voltage phase angle differences considering the other phase angles θ_{11}, θ_{14} , θ_{23} and θ_{31}as the reference, one at a time is presented in Table 2.3.

Table 2.3 Summary of results for DT training accuracies for single reference AD approach

Reference Angle	**Accuracy**
θ_1	98.29
θ_{11}	99.57
θ_{14}	98.29
θ_{23}	99.14
θ_{31}	99.14

From Table 2.3, we observe that the accuracy of DT for the training data is dependent on the reference voltage phase angle selected. Thus, in the single reference angle difference approach, the accuracy depends on a single reference's location and signal quality [75]. It is also at times prone to large non-detection zones or mal-operations and lower accuracies [20]-[35].

Multiple reference approach [35]: Total number of PMUs for the modified 18 bus test system are 5 and considering two pairs of phase angles at a time, we will have C_2^5 i.e. 10 combinations of relative voltage phase angle differences. Multiple reference approach uses more than one reference signal from multiple locations around the network and is more robust. Comparing accuracies from Tables 2.3 and 2.4, we observe that this approach has higher accuracies as compared to the single reference approach. This approach is therefore selected for comparison with the proposed *CUSPAD* approach.

Table 2.4 Summary of results for DT training accuracies for multiple reference AD approach

Sl no.	Reference Angle	Accuracy
1	$Multiple\ references$	99.79

Now to test the DT model, the simulations were repeated 50 times and a 95% confidence interval accuracy was computed for the test data with a range of measurement errors consisting of both PMU and instrumentation channel errors. It can be observed from Table 2.5 that the accuracy of AD for the 30th measurement sample is significantly affected by measurement errors.

Comparing Tables 2.2 and 2.5, it can concluded that the CUSPAD approach is not affected significantly by measurement errors while that of the multiple reference AD approach is affected by the same. The DT results for both approaches are depicted in Figures 2.16 and 2.17. The red terminal nodes denote islands while the blue terminal nodes denote non-islands. Based on the performance of this approach in the modified 18 system, the performance of the proposed approach is now tested on the 118 bus system in the next section.

Table 2.5 Summary of results for DT testing accuracies with multiple reference AD approach considering measurement errors

Error		AD	
Systematic Error	**Random Error**	**Accuracy (95%)**	**Depth**
0	0 Mean ±0.104 SD	99.79±0.00	5
0 Mean ±0.1 SD		99.37±0.06	5
±1		96.85±0.51	5
±2		94.66±0.68	5
±4		93.04±0.8	5

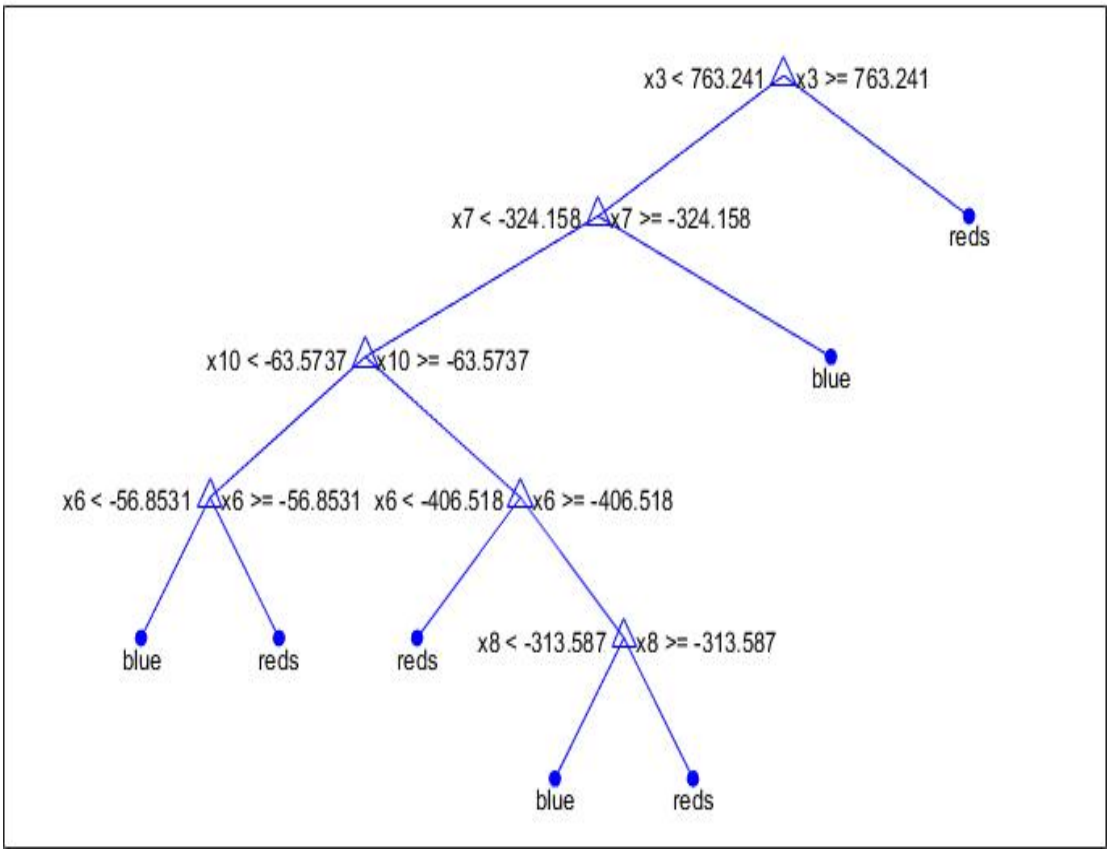

Figure 2.16: DT results for 18 bus system using CUSPAD approach

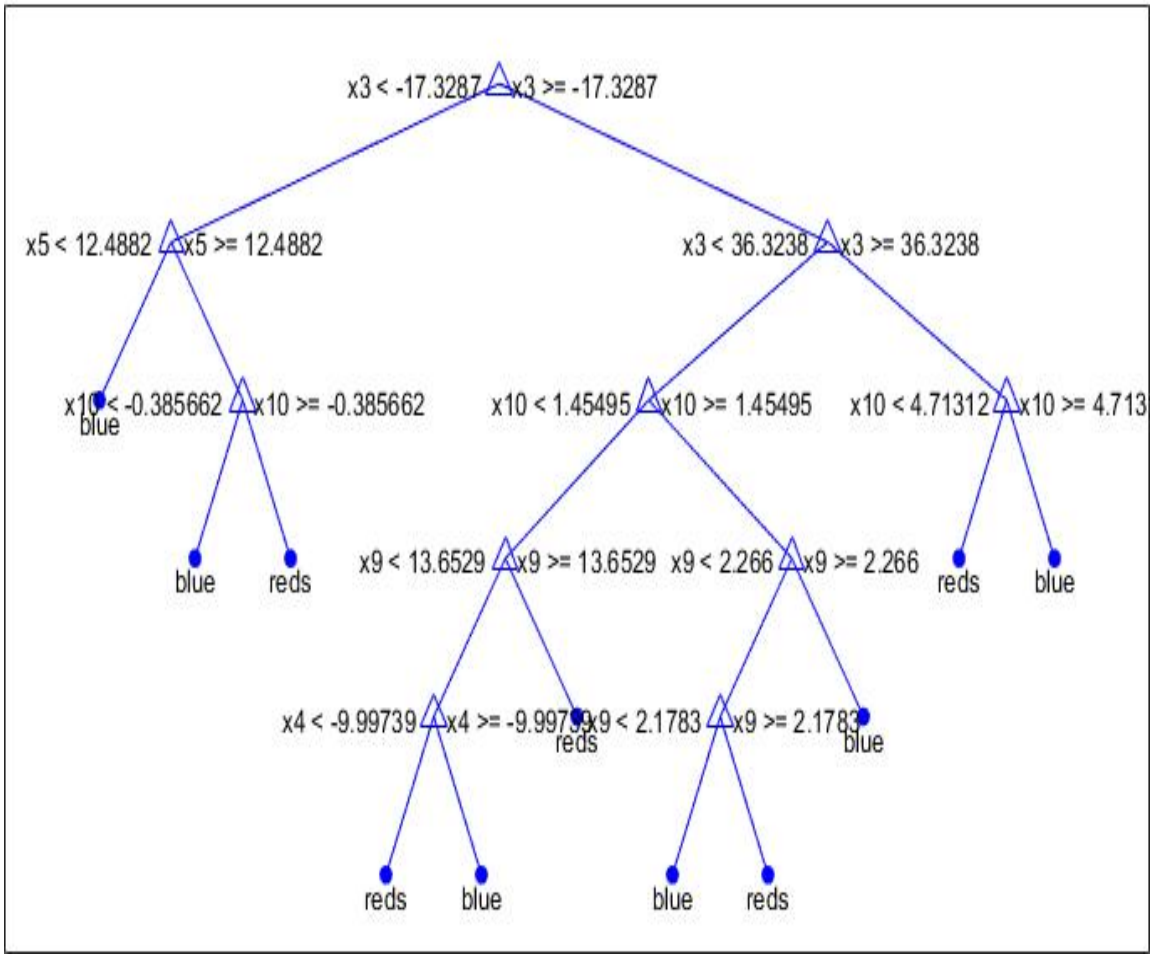

Figure 2.17: DT results for 18 bus system using AD approach

2.4.6. Simulation and Results for modified 118 bus case

Case 2: 118 Bus Test Case:

The original IEEE 118 bus system is modified to include various percentages of wind energy penetration in the network by replacing some of the conventional generators with an equivalent capacity aggregated wind farm connected to the 132 kV network. The original system is comprised of 118 buses, 54 generators, 177 transmission lines and 9 transformers. The real power generation of the system and electrical load is approximately 3793 MW and 3668 MW, respectively.

Database:

To build the database for the islanding detection algorithm several non-islanding scenarios are analyzed such as faults, line trips, generator trips, transformer trips and generation load mismatch. To generate islands in the 118 bus system, a community based islanding partitioning logic [73] is used. It is considered that an electrical network can be depicted using graph theory, where each bus is represented by a node, n, and transmission lines or transformers are denoted by edges, e. A community is a cluster of nodes which have high connectivity within itself but few connections outside it. In Figure 2.18, the intra-community edges between the communities are denoted by solid black lines while the inter-community edges, which is those within each community are denoted by dotted black lines. By identifying and eliminating the inter-community edges, the network is divided into islands.

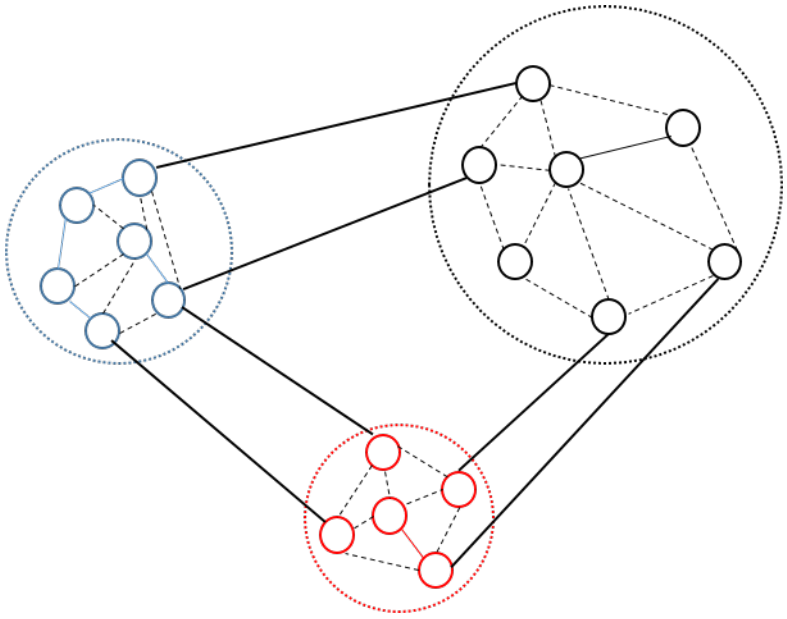

Figure 2.18: Representation of communities in a graph [73]

An algorithm is developed in [73] which identified the number of edges that need to be terminated to form islands. In this algorithm, the highest weight is assigned to the inter-community edges. Once the edge identified with the highest weight is removed, a

clustering algorithm is run which identifies nodes within a community and checks for creation of islands. If all the nodes are clustered in the same group, an island has not been formed and an edge with the next highest weight is identified and removed until the desired number of islands are formed. To create the islanding scenarios in the 118 bus system, islands having a maximum of 9 nodes aRE created by removing branches one after another at different instants of time. In total, 2000 cases were simulated for each level of wind penetration, namely 10%, 20% and 30% wind generation, each of which comprised of 1000 islanding and 1000 non-islanding cases, respectively.

PMU locations:

The total number of PMUs required for complete observability of this system were found in accordance with the formulation described in Section 2.4.4. The 38 PMUs were located on buses 3, 5, 8, 9, 12, 15, 17, 21, 23, 28, 30, 36, 40, 43, 45, 49, 52, 56, 59, 63, 65, 66, 68, 69, 71, 75, 77, 80, 85, 86, 84, 91, 94, 101, 105, 110, 114, and 116.

Window size:

Since a window size of 30 samples yields high accuracies for the 18 bus system, the same window size is considered for running simulations for the 118 bus system.

a. Case 2 a. About 10% of the total generation is replaced with wind turbines and the accuracy of the scheme is tested on this modified system. The simulations were repeated 50 times and a 95% confidence interval accuracy was computed for the test data with a range of measurement errors. The results obtained are presented in Table 2.6

Table 2.6 Summary of results for AD and CUSPAD accuracies with measurement errors for 10% wind penetration

Error		Angle Difference		CUSPAD	
Systematic Error	**Random Error**	**Accuracy (95%)**	**Depth**	**Accuracy (95%)**	**Depth**
0	0 Mean ±0.104 SD	99.45±0.00	3	99.65±0.00	3
0 Mean ±0.1 SD		94.14±0.60	3	94.64±.80	3
±1		78.70±1.10	3	94.84±0.86	3
±2		74.70±1.95	3	94.48±0.91	3
±4		70.98±3.07	3	94.46±1.04	3

b. Case 2b: Modified 118 bus: About 20% of the total generation is replaced with wind turbines and the accuracy of the scheme is tested on this modified system. The simulations were repeated 50 times and a 95% confidence interval accuracy was computed for the test data with a range of measurement errors. The results obtained are presented in Table 2.7.

Table 2.7 Summary of results for AD and CUSPAD accuracies with measurement errors for 20% wind penetration

Error		AD		CUSPAD	
Systematic Error	**Random Error**	**Accuracy (95%)**	**Depth**	**Accuracy (95%)**	**Depth**
0	0 Mean ±0.104 SD	98.80±0.00	3	99.70±0.00	3
0 Mean ±0.1 SD		92.51±0.69	3	98.90±0.60	3
±1		76.03±2.37	3	98.99±0.62	3
±2		67.70±3.48	3	98.82±0.59	3
±4		62.54±3.95	3	98.91±0.95	3

c. Case 2c: About 30% of the total generation is replaced with wind turbines and the accuracy of the scheme is tested on this modified system. The results obtained are presented in Table 2.8 and Figures 2.19 and 2.20.

Table 2.8 Summary of results for AD and CUSPAD accuracies with measurement errors for 30% wind penetration

Error		AD		CUSPAD	
Systematic Error	**Random Error**	**Accuracy (95%)**	**Depth**	**Accuracy (95%)**	**Depth**
0	0 Mean ±0.104 SD	99.8±0.00	4	99.80±0.00	4
0 Mean ±0.1 SD		93.45±2.79	4	99.20±0.14	4
±1		78.40±2.12	4	99.24±0.147	4
±2		69.06±2.40	4	99.22±0.15	4
±4		66.18±3.12	4	99.22±0.146	4

In Figures 2.19 and 2.20, the red terminal nodes denote islands while the blue terminal nodes denote non-islands. From Figures 2.16 and 2.17 and Tables 2.6, 2.7 and 2.8, it can be observed that the accuracy of angle difference of phase angles for the 30th sample decreases as the measurement error increases for the 118 bus test case with varying percentage of wind energy penetration. In contrast the cumulated sum approach is not affected by presence of errors for the same depth of DT for all the cases.

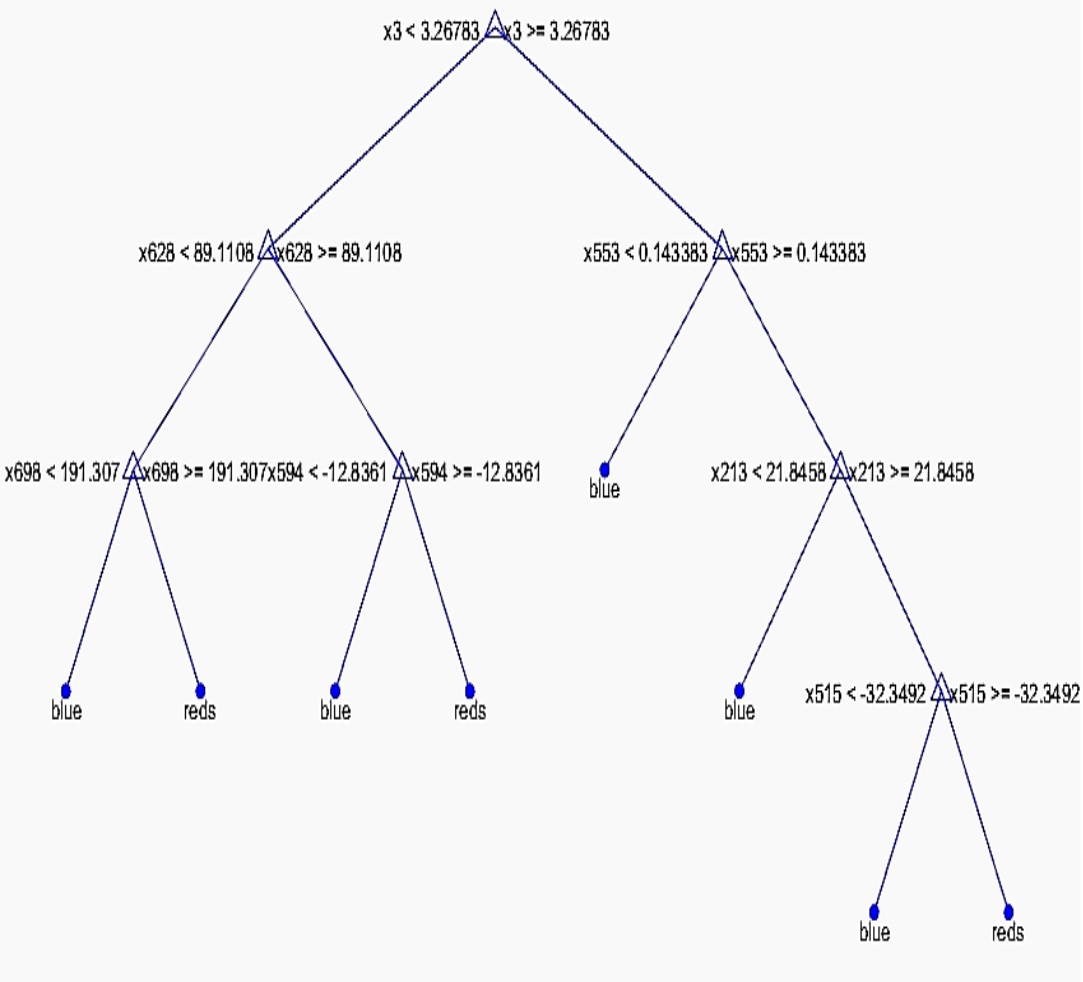

Figure. 2.19: DT result for 118 bus system using CUSPAD approach with 30% wind

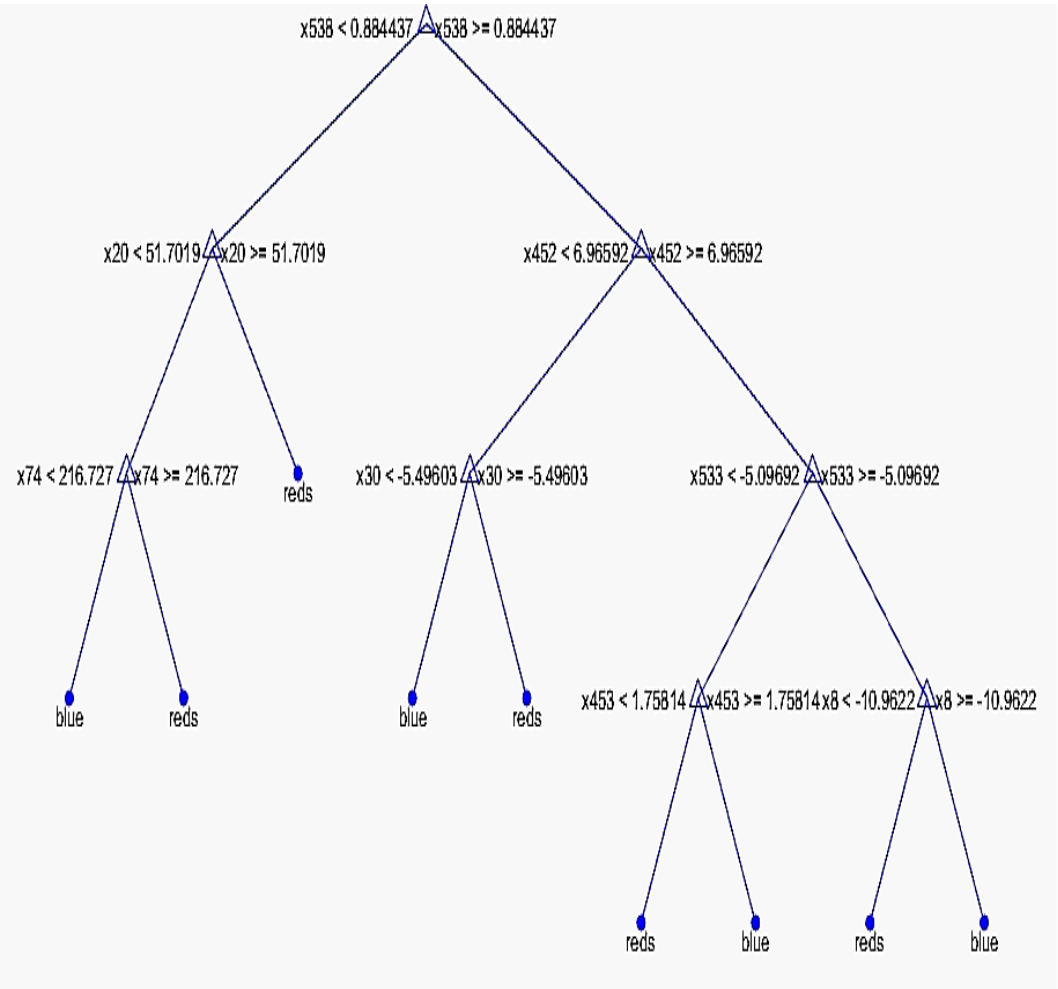

Figure. 2.20: DT result for 118 bus system using AD approach with 30% wind

2.4.7. Discussion and Conclusion

Discussion

1. The performance of the proposed algorithm has been tested offline but to implement this in real time, the preprocessing of voltage phase angles would be required as discussed in Section 2.4.3.
2. The performance of the algorithm has been tested for various wind energy penetration, but the influence of wind dynamics in an electrical network has not been specifically studied in this research work.

Conclusion

In this chapter, an islanding detection technique is proposed and tested. When an island is formed and the isolated system loses observability of the grid and vice versa, the accuracy of the proposed technique is not affected. This approach has been tested for an 18 bus test system using DT based CART classifier and the performance results for the proposed Cumulative Sum of Phase angle Difference (CUSPAD) technique is observed to be better in presence of measurement errors as compared to that of the conventional relative angle difference (AD) of phase angles. The performance is further tested for the 118 bus system where varied levels of wind penetration is modeled in the transmission system. It is found that with varying levels of wind energy penetration, the performance accuracies for the CUSPAD approach are superior in presence of measurement errors of as compared to that of the AD approach.

CHAPTER 3[2]

OUTAGE ANALYSIS AND RELIABILITY EVALUATION OF THE BULK TRANSMISSION SYSTEM

Reliability metrics are used for measuring reliability of any system. The power industry uses several metrics to quantify the distribution system reliability such as SAIDI, SAIFI, CAIDI and CAIFI. However, reliability indices used in the industry for the transmission system are not numerous. In this chapter, reliability of the transmission system is evaluated on the basis of metrics available in the literature and the existing standards. A new metric is also proposed in this chapter which measures reliability of the transmission network on an annual basis using both outage frequency and duration. This metric can further evaluate severity of transmission line outages on the basis of outage category using historical transmission outage data.

3.1. Background

3.1.1. Transmission System Reliability

The ability of the power system to perform its required function within a specified time frame and meet the expected performance criteria is termed as reliability[76]. According to the North American Electric Reliability Corporation (NERC), the definition of reliability of the Bulk Power System (BPS) is the ability of the system to withstand disturbances and meet consumer demands consistently [77]. Reliability of the transmission system ensures secure transfer of uninterrupted power from the generating sources to the load centers and is thus of utmost importance to both utilities and

[2] This chapter is based on a publishable work

consumers. Unreliability of the bulk transmission system may lead to cascading failures resulting in brownouts or blackouts.

Reliability of the transmission system can be measured in terms of frequency, duration, and magnitude of damage caused by transmission line outages [78]. Quantitative evaluation of reliability is a crucial component during planning, design, operation, and maintenance phases of the power system [79]. Furthermore, detailed analysis of system reliability may reveal vulnerable areas in the transmission network and establish a chronological system performance that would serve as a guideline for future reliability assessment[76].

3.1.2. Motivation and Objectives

For measurement of the existing power system performance and assessment of its performance in the future, a reliability metric is the primary requirement [78]. In the literature, the distribution system reliability can be evaluated with the help of numerous reliability metrics such as System Average Interruption Frequency Index (SAIFI), System Average Interruption Duration Index (SAIDI), Consumer Average Interruption Frequency Index (CAIFI), Consumer Average Interruption Duration Index (CAIFI), and Average Service Availability Index (ASAI) [80]. These distribution system reliability indices measure frequency and duration of distribution system outages as a function of the number of customers affected. However, in the transmission system, such indices cannot be used to evaluate system reliability because consumers are not (typically) directly affected by a transmission line outage. Therefore, there is a need to develop a reliability metric which can comprehensively measure the reliability of the transmission network.

The objectives of this research work can be enumerated in the following way:
1) Development of a composite transmission reliability metric, and 2) Transmission line outage analysis incorporating outage frequency and duration for establishing baselines.

The proposed metric can be used by utilities to identify and prioritize risks and take corrective actions, if found necessary.

3.2. Literature Review

3.2.1. Existing metrics

Transmission reliability indices are used to monitor and provide a quantitative measure of the transmission system performance. In [81]-[85] emphasis has been laid on quantitative evaluation of transmission reliability using historical transmission line outage data and probability theory. As per IEEE Std. 859:1987- IEEE Standard Terms for Reporting and Analyzing Outage Occurrences and Outage States of Electrical Transmission Facilities [81], the outage indices used for transmission system performance evaluation are classified as:

- Rate Indices: Outage and Failure rate
- Duration Indices: Mean Time to Outage and Mean Outage Duration
- State Probability Indices: Availability and Unavailability

Additionally, IEEE Std. 493:1997- IEEE Recommended Practice for the Design of Reliable Industrial and Commercial Power Systems (Gold Book) [82] provides information on key performance indices used for power system reliability analysis such as Mean Time Between Failure (MTBF) and Mean Time To Repair (MTTR). In 2008, NERC approved the Transmission Availability Data System (TADS) to collect transmission equipment inventory and outage data. These data were used by NERC committees to analyze transmission line outages [83], [84].

3.2.2. Gaps in Literature

In [5] a new statistical analysis model was proposed that considered the stochastic nature of outages and classified the variables into three groups, namely, categorical, indicator, and explanatory. A new index called Severity Factor was introduced in [5] to

prioritize failure causes over the entire study period by using outage frequency and duration. But this metric was not found to be useful during evaluation of outage severity on an annual basis, as demonstrated in Section 3.5. From [3] it is observed that a continuing need exists to formulate suitable approaches to evaluate and verify transmission system performance in the industry. Therefore, in this chapter, a comprehensive overview of transmission reliability metrics based on IEEE standards, prior research, and industrial practices is also presented.

Forced Outage per Hundred Miles per Year (FOHMY) is a transmission reliability index which is widely used in the electric power industry. FOHMY, also known as Circuit Outage Frequency per 100 Circuit Miles, is an annual ratio that relates the number of forced outages to the circuit mileage of the line [83], and is given by

$$FOHMY[83] = \frac{Total\ Forced\ Outage\ Frequency * 100}{Circuit\ Miles} \quad (3.1)$$

It is well-known that both frequency and duration of transmission line outages have significant impacts on operation and reliability of the power system [3] However, FOHMY does not take into account outage duration in its formulation, and thus it may not be a good representation of the transmission reliability if used on its own. In Section 3.4 both negative and positive correlation of FOHMY with some of the other performance indices discussed in the literature are observed. This is elaborated further in Sections 3.4.1 and 3.5.

3.3 Transmission Network Outages

Nearly a decade worth of transmission outage data and related statistics from a U.S. power utility is used for carrying out this research work. These data have been used to analyze outages, access past system performance, and develop metrics that would give a comprehensive assessment of transmission reliability. In this chapter, the transmission

system performance and reliability are evaluated based on the historical forced outage data for the 69-500 kV voltage levels for the time-period 2009-2016.

3.3.1. State of a Transmission Line

The state of a transmission line refers to whether it is available or unavailable [81]. When a transmission system is available, it means it is available for operation but can either be in-service or turned off. These decisions are made by the utility operating the transmission lines. On the other hand, when a transmission system is unavailable, the transmission line cannot be energized. The line is either unavailable because of a forced outage or is scheduled for planned maintenance activities. In such cases, it is said that the transmission line is under planned outage. A forced outage occurs against a utility's planning and may occur due to a fault in the system or as an emergency operating scenario. These conditions can further be classified as illustrated in Figure. 3.1.

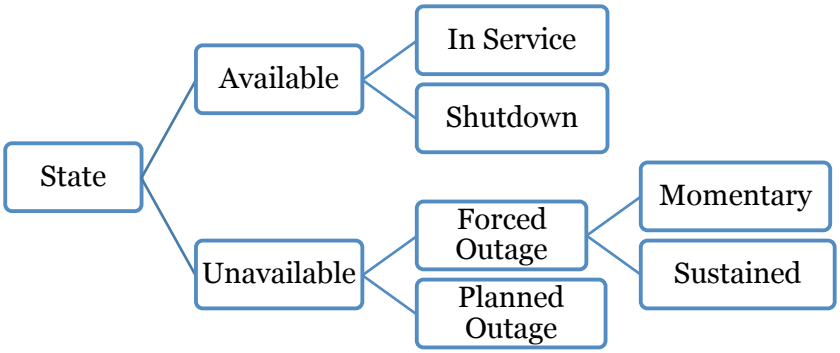

Fig 3.1: States of a transmission line considered in this analysis

3.3.2. Outage Classification

The term outage refers to the state of a transmission line when it is not-in-service or is de-energized. As per [81], outages can be classified as forced outages and scheduled (planned) outages. A forced outage is automatic or manual in nature and cannot be deferred due to operational or safety constraints. Conversely, a scheduled (planned)

outage is intentional and manual and can be deferred without risk of damage to equipment or human life. Forced outages can be further classified based on duration as [83]:

- Momentary Outage: Outage duration of less than 1 minute (usually restored by an auto reclosing line post-fault [77]).
- Sustained Outage: Outage duration of 1 minute or longer.

Both types of forced outages, that is, momentary and sustained, have been considered in this analysis.

3.3.3. Outage Categories

Transmission line performance depends on a variety of factors ranging from malfunctioning of power system components to environmental conditions, such as storms. The power industry broadly categorizes transmission outages as : 1) equipment; 2) system protection; 3) lines; 4) weather; 5) lightning; 6) unknown; 7) external; 8) others; and 9) human factors. These categories are further coded into outage subcategories as described in Table 3.1 and the abbreviations are expanded in Table 3.2.

Table 3.1: Coding of outage categories into outage cause codes

Sl. No.	Outage Category	Outage Cause
1	Equipment	AC, BK, SU, VA
2	System Protection	CO
3	Lines	PO, XF
4	Weather	WI, ST
5	Lightning	LI
6	Unknown	UN, KV,FT
7	External	PC, FS, KV
8	Other	HU, AN,AU, BI, CN, DE, FI
9	Human Factors	IP, SP

Table 3.2: Expansion of outage cause code abbreviations

Abb.	Description	Abb.	Description
AC	AC Circuit Equipment	KV	Underbuilt Line
AN	Animals	LC	Shunt Capacitor or Reactor Failure
AU	Vehicle Caused	LI	Lightning
BI	Bird Contact	PC	Power System Condition
BK	Breaker Failure	PO	Pole Failure
CN	Contamination	SP	Inadvertent By Utility
CO	Communications, Control, Relay	ST	Storm
DE	Debris in Equipment	SU	AC Substation Equipment Failure
FI	Fire	UN	Unknown
FS	Foreign System	VA	Vandalism
FT	Fault	XF	Transformer Failure
HU	Inadvertent By Public	WI	Wind
IP	Inadequate Procedures		

3.4. Outage and Reliability Analysis

An outage in the transmission network is detrimental as it can lead to a reduction in transfer path redundancy and/or capacity. Furthermore, the outage duration, which indicates the time for which the line is unavailable, may vary, ranging from less than a minute to several hours [17]. Therefore, while evaluating the performance of the transmission network using outage data, it is relevant to consider the failure rate, referred henceforth as outage frequency as well as the duration for which the line has been unavailable, referred henceforth as outage duration. In this section, outage analysis and reliability evaluation of the transmission network performance based on existing indicators described in IEEE standards and TADS is carried out.

3.4.1. Outage Analysis based on TADS Reliability Metrics

In 2008, NERC approved implementation of TADS Phase I which required U.S. Transmission Owners to report automatic outages beginning 2008 for AC circuits >= 200 kV. According to [83], [84] some of the reliability metrics developed for reporting transmission outages were:

- Outage frequency per 100 Circuit Miles (equivalent to FOHMY)
- Total Element Outage Frequency (TOF)
- Total Element Outage Duration (TOD)
- Mean Time Between Failure (MTBF)
- Mean Time To Repair (MTTR)
- Availability

For a preliminary analysis of performance adequacy representation of FOHMY in terms of outage frequency and duration, a comparison between FOHMY and TADS metrics TOF and TOD is made. From Figure 3.2, it is observed that FOHMY and TOF have a positive correlation as both are a representation of the outage frequency. However, from Figure 3.3, it is observed that while the FOHMY value for 2009 was greater than that in 2012, 2014 and 2015, the outage duration (TOD) for 2009 is lower than the TOD values for these three years. Thus, it can be concluded that FOHMY cannot capture the impact of the outage duration and would therefore not give an accurate representation of transmission line outage severity in its entirety. This is due to the fact that FOHMY definition is not inclusive of the outage duration. The definitions of TOF and TOD [83] are given below.

- Total Element Outage Frequency (TOF) is a representation of the outage frequency per transmission element per year and is mathematically defined by (3.2).
- Total Element Outage Duration (TOD) is a representation of the outage hours per transmission element per year and is mathematically defined by (3.3).

The remaining TADS metrics such as MTBF, MTTR and Availability are described in the next section.

$$TOF[83] = \frac{Total\ Outage\ Frequency}{Total\ Elements} \tag{3.2}$$

$$TOD[83] = \frac{Total\ Outage\ Duration}{Total\ Elements} \quad (3.3)$$

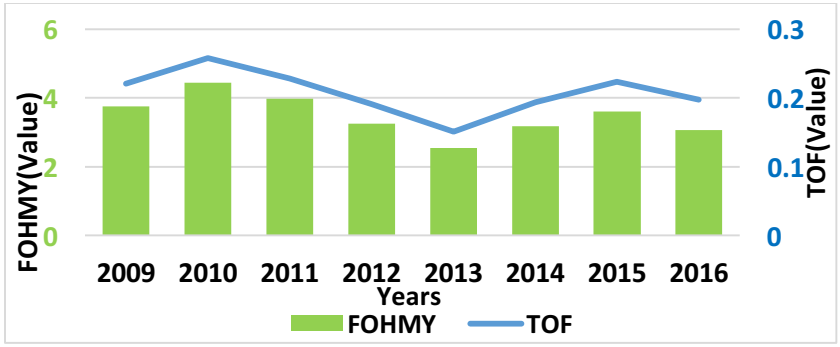

Fig 3.2: FOHMY vs. TOF (69-500 kV)

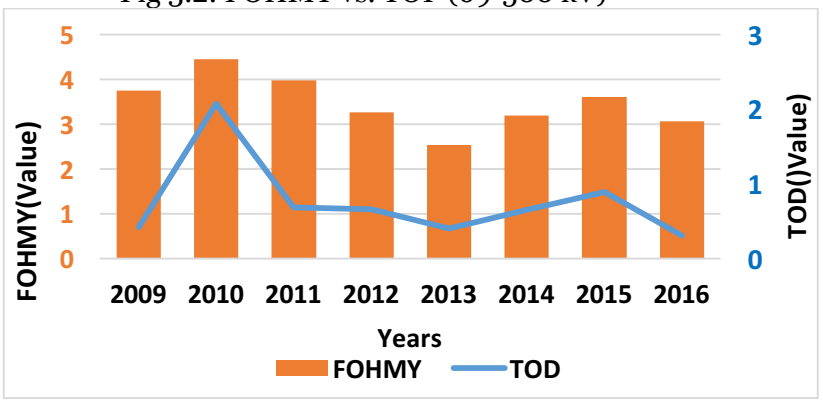

Fig 3.3: FOHMY vs. TOD (69-500 kV)

3.4.2. Outage Analysis based on Outage Frequency

Forced outages such as sustained and momentary outages are considered for this analysis. Outages have been analyzed on the basis of frequency of occurrence and have been classified according to their operating voltage level. This is represented in Figure 3.4 where it is observed that the overall frequency of forced outages is highest for 69 kV, followed by 115, 230 and 500 kV, respectively. It is also observed that the percentage of sustained outages are higher as compared to momentary outages for each voltage level. Frequencies of both momentary and sustained outages are observed to be highest for 69 kV lines followed by the 132 kV lines.

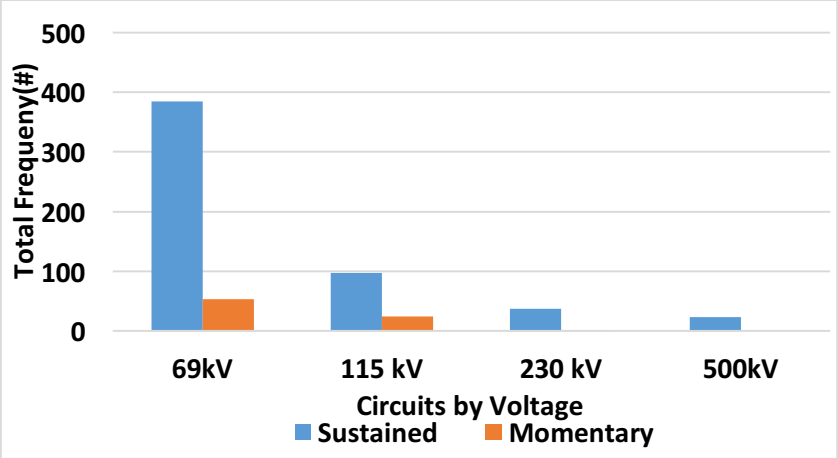

Fig 3.4: Outage Frequencies (69-500 kV)

- The Annual Outage Rate (AOR) provides the annual outage rate of the transmission system specific to a voltage class and is mathematically defined by (3.4), and visually depicted by Figure 3.5. Exposure time in (3.4) is considered to be 1 year. From Figure 3.5, it is observed that AOR is highest for 69 kV, followed by 115 kV. The annual outage rates of 69 kV are observed to be nearly constant at around 60 outages per year except in 2012-2013 when the rate was observed to have decreased. For 115 kV, the trend is observed to be on a decrease in general except for peaks observed in 2013 and 2015. The AOR value for 115 kV was observed to be around 20 outages or less per year. AOR for 230 and 500 kV lines is observed to be in general low at around less than 10 outages at an average per year.

$$AOR\ [82] = \frac{Total\ Outages\ Frequency}{Exposure\ Time} \qquad (3.4)$$

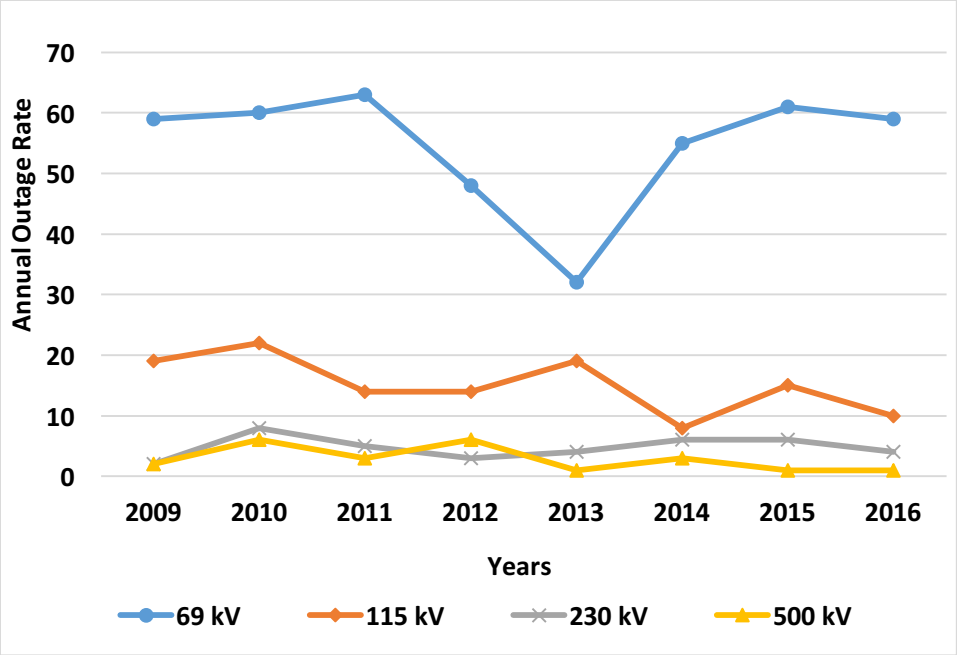

Figure 3.5: Annual Outage Rate (AOR) Trend

- The Total Element Outage Frequency, TOF, described above is mathematically represented by (3.2) and visually depicted in Figure 3.6. It depends on the total number of elements in a particular voltage level, so it essentially provides a comparison of the total number of outages as a percentage of the total elements in that particular voltage level. This is helpful in comparing the outage severity for each voltage level with respect to the total number of elements. It is observed from Figure 3.6 that TOF for 69, 230 and 500 kV is lower than that for 115 kV. The TOF for 115 kV is observed to be around 1 in the year 2009 and 2013 but it has been observed to be comparatively lower in the remaining years under study. The TOF for 69, 230 and 500 kV is observed to be lower than 0.4 for the years considered in this analysis.

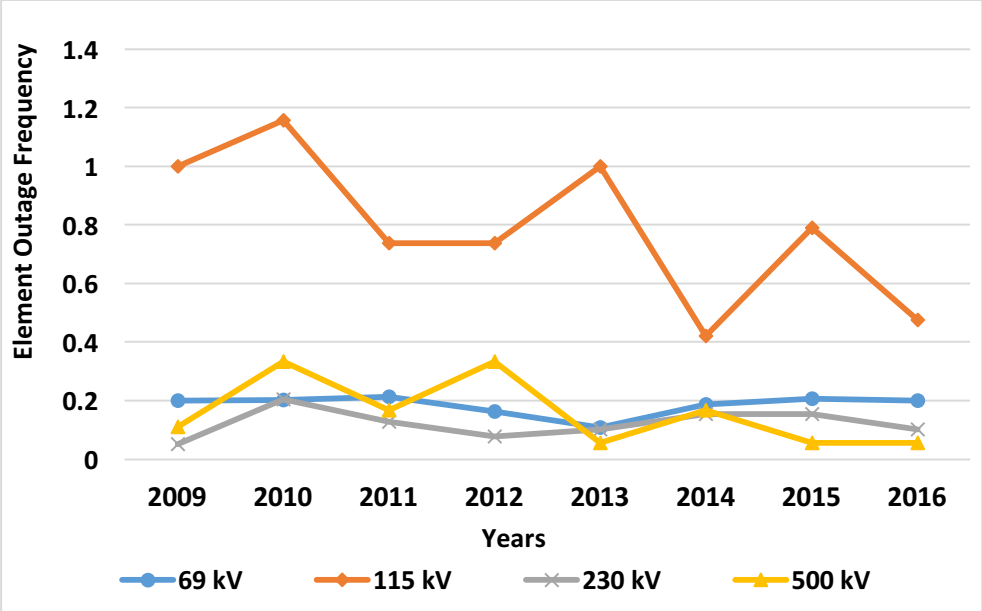

Figure 3.6: Total Element Outage Frequency (TOF) Trend

3.4.3. Outage Analysis based on Outage Duration

- The Annual Outage Duration (AOD) provides the annual outage duration of the transmission system specific to a voltage class. It is mathematically defined by (3.5) and visually depicted by Figure 3.7. Exposure time in (3.5) is assumed to be 1 year. From Figure 3.7, it is observed that AOD for 69 kV is the highest followed by 115, 230 and 500 kV, respectively. The annual rate of 69 kV is also observed to follow a decreasing trend in general except between 2013-2015. For higher voltage levels, the trend is observed to be decreasing in general except for peaks in 2012 (500 kV), 2013 (115 kV) and 2016 (230 kV). In general over the study period, the AOD for the entire 69 kV network is observed to be above 100 hours per year while that for 115 kV is observed to be at an average of 50 hours per year. AOD for 230 and 500 kV is observed to be insignificant as compared to 69 and 115 kV, however we observe a peak in AOD for 500 kV lines in the year 2012.

$$AOD[82] = \frac{Total\ Outage\ Duration}{Exposure\ Time} \qquad (3.5)$$

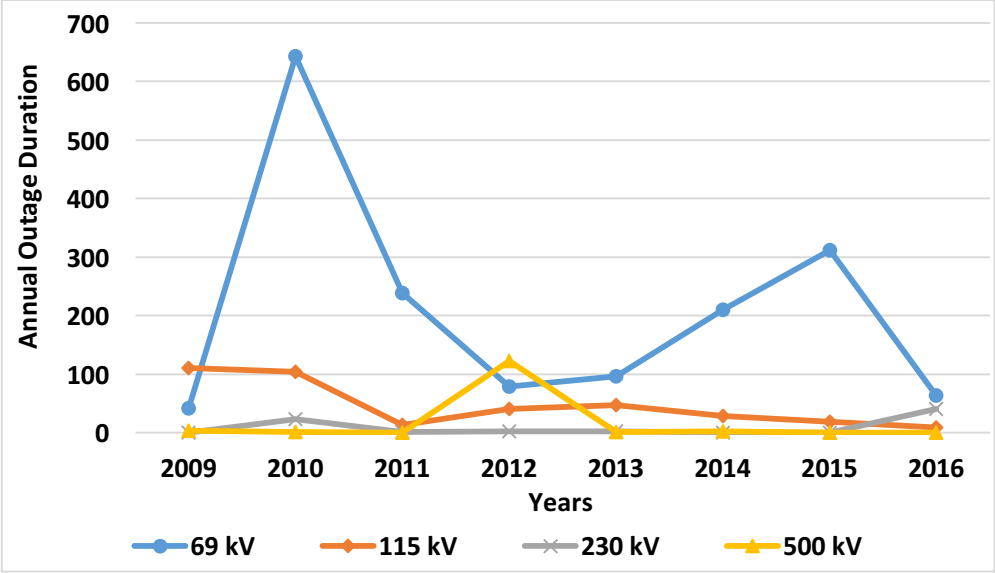

Figure 3.7: Annual Outage Duration (AOD) Trend

- Total Element Outage Duration, TOD, is mathematically defined by (3.3) and visually depicted in Figure 3.8. Exposure time in (3.3) is assumed to be 1 year. From Figure 3.8, it is observed that TOD is lowest for 500 kV except for the year 2012 and highest for 115 kV, in general. The TOD is the outage hours per transmission element per year and 69 kV values are lower than 115 kV followed by 230 kV. This metric depends on the total number of elements in a particular voltage level, so it essentially provides a comparison of the total outage duration as a ratio of the total elements in that particular voltage level. This is helpful in comparing the outage severity with respect to the total duration for which the element is outaged for each voltage level. It is observed from Figure 3.8 that TOD for 69, 230 and 500 kV is lower than that for 115 kV. The TOD for 115 kV is observed to be at an average of 2 hours a year except for peaks in 2009 and 2010. The TOF for 69, 230 and 500 kV is observed to be lower than 2 hours throughout the study period. However a peak in TOD in the year 2012 for the 500 kV lines can be observed.

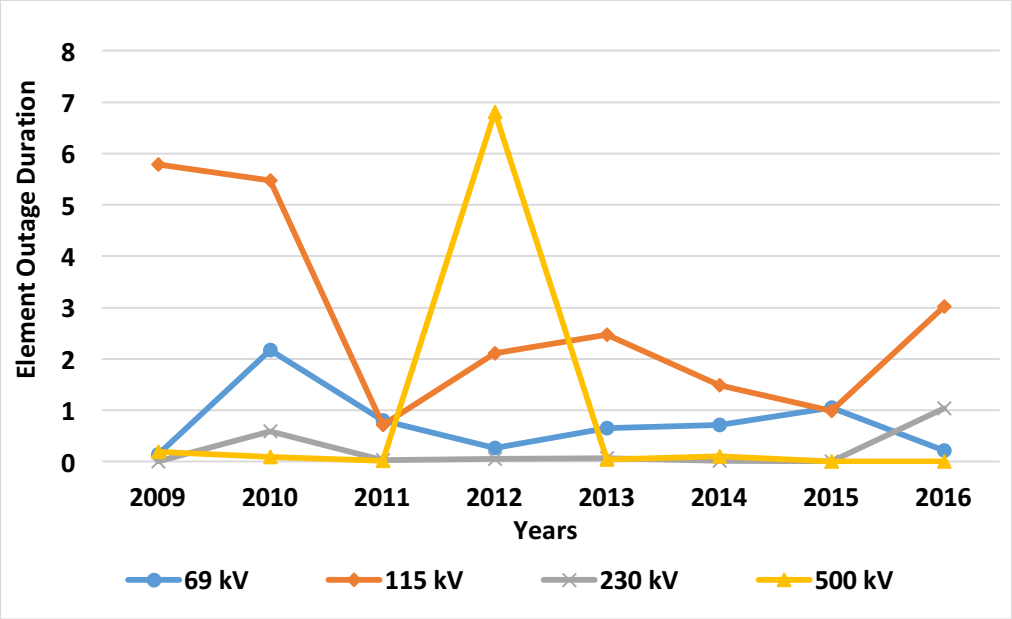

Figure 3.8: Total Element Outage Duration (TOD) Trend

3.4.4. Reliability Analysis based on Operation Performance

Maintainability and availability are parameters used for specification of system design and as indicators of operational performance [82]. They are closely related to and contribute towards system reliability. The mathematical formulations have been obtained from [82].

- Mean Time Between Failure: Mean Time Between Failure (MTBF) is a basic measure of the reliability of a system and determines the average time elapsed between two failures. It is denoted by (3.6) and depicted visually in Figure 3.9. From Figure 3.9, it is observed that MTBF is highest for 500 kV followed by the lower operating voltage lines. Higher values of MTBF are desirable as they indicate a lower number of failures within a specified period. Exposure time in (3.6) is 8760 hours (=1 year).

$$MTBF\ [82] = \frac{Exposure\ Time}{Total\ Outages} \tag{3.6}$$

- Mean Time To Repair: Mean Time To Repair (MTTR) indicates the efficiency of corrective action taken to restore an outaged line and is dependent on a variety of factors, such as human skills, environment, etc. MTTR is denoted by (3.7) and depicted visually in Figure 3.10. From Figure 3.10, it is observed that MTTR for 69 kV is the highest and it is lower for higher voltages which is desirable as it indicates better maintainability. However, a peak in MTTR was observed for 500 kV in 2012 and for 230 kV in 2016. Low values of MTTR are desired because it indicates efficient repair works.

$$MTTR[82] = \frac{Outage\ Duration}{Total\ Outages} \tag{3.7}$$

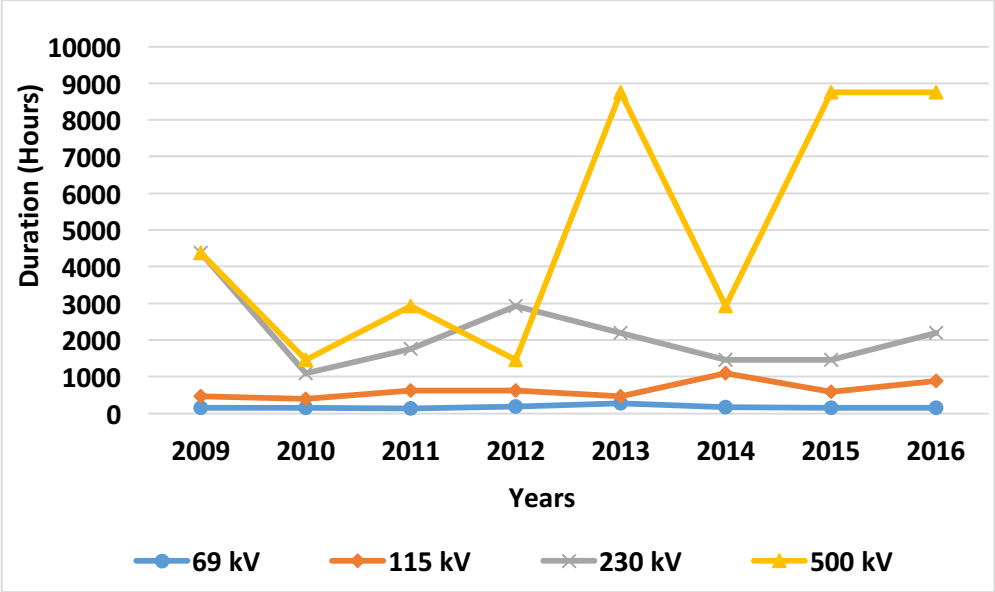

Figure 3.9: Annual MTBF Trend

- Availability: Availability is a mathematical representation of the percentage of time for which a system is available and ready for use [82]. It is denoted by (3.8) and visually depicted by Figure 3.11.

$$Availability[82] = \frac{MTBF}{MTBF + MTTR} \tag{3.8}$$

From Figure 3.11, it is observed that availability of the transmission lines rated higher than 69 kV is more than 97% throughout the study period. For 69 kV, the availability was observed to be above 97% except for the years 2010 and 2015. Thus, the overall availability of the transmission network under study is very high. Based on the outage analysis and reliability evaluation done above, a chronological trend in outage duration and frequency can be established. This can then become the basis for future reliability assessments.

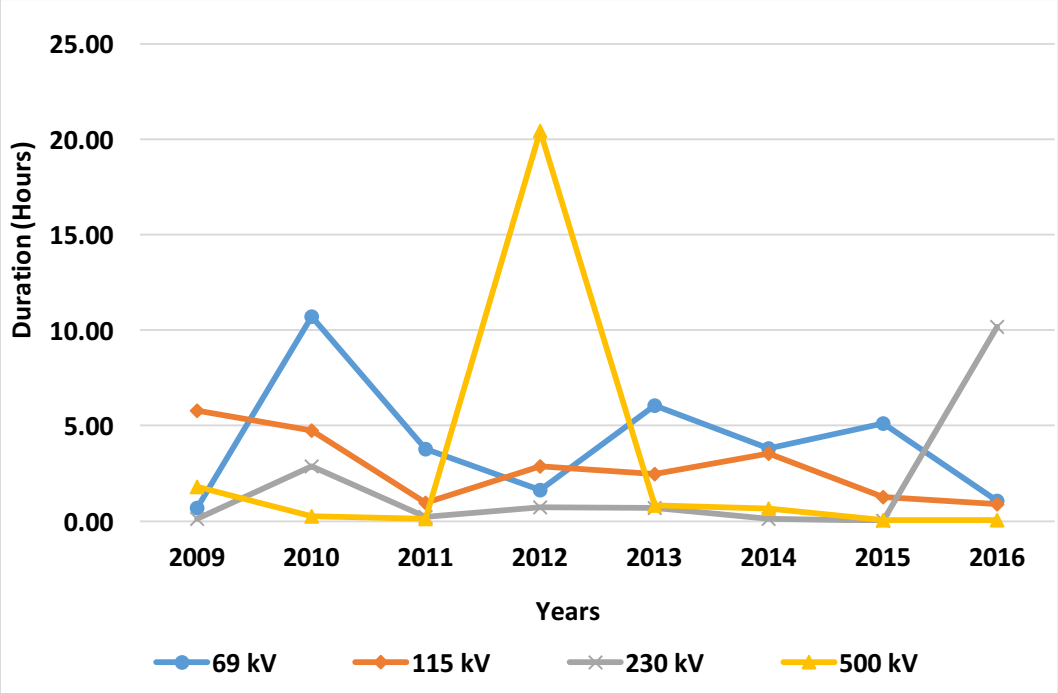

Figure 3.10: Annual MTTR Trend

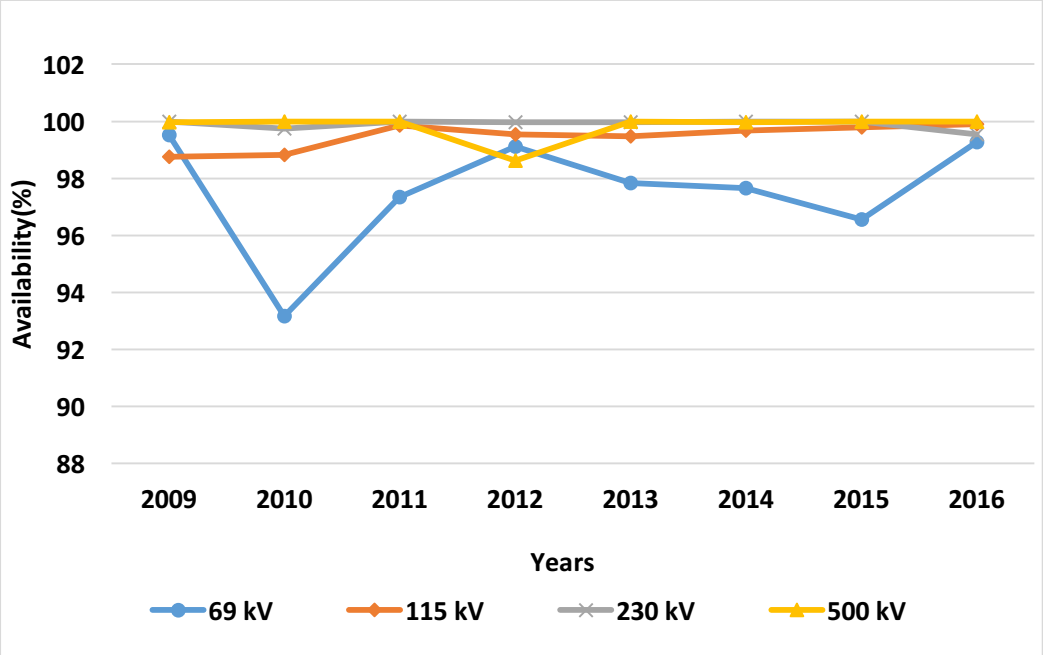

Figure 3.11: Annual Availability

3.5 Outage Category Prioritization

Outage categories have been listed in Table 3.3 based on the longest outage duration as well as the maximum/minimum frequency of occurrence. It is observed from this table that the longest outage duration category may not correspond to the most frequently occurring outage category. Hence, focusing only on the number of outages (which is what FOHMY does) would provide information regarding the outage frequency and not the outage duration. As such, it may not be possible to distinguish between two contrasting situations where frequent outages are characterized by lower interrupted durations, as is observed in Table 3.3 for 69-230 kV lines. To cite an example, for 69 kV lines, it is observed that wind-related outages (WI) are of the longest duration while Debris in Equipment (DE) occur most frequently. Therefore, as the most frequent outage type is not necessarily the one that has the longest duration, both frequency and duration should be considered as independent indicators of transmission reliability. This inference

becomes the basis of the formulations for Susceptibility Index (SI) and Outage Impact Index (OII) described below.

Table 3.3: Outage classification on maximum duration and frequency

Circuit Voltage	Longest Duration	Most Frequent	Least Frequent
69 kV	WI	DE	IP, LC, VA*
115 kV	ST	LI	XF, AU, KV*
230 kV	AC	SP, BI*	XF, FT, SU*
500 kV	FS	FS	XF, BK, FT*

* Multiple entries indicate equal frequency of occurrence

3.5.1. Susceptibility Index (SI)

Susceptibility Index (SI), derived from Severity Factor of [5], for an outage category α and voltage level V (69, 115, 230 or 500 kV) is given by

$$SI_{\alpha,v} = \frac{N_{\alpha,v}}{N_v} * \frac{IT_{\alpha,v}}{IT_v} \tag{3.9}$$

where, $N_{\alpha,v}$ is the number of outages for category α and voltage v , N_v is the total number of outages for voltage level v, $IT_{\alpha,v}$ is the outage duration for category α and voltage v, and IT_v is the total outage duration for voltage level v. This comprehensive index identifies the most severe outage category by comparing the outage category's (α) frequency and duration to the total outage frequency and duration for the voltage class v.

SI values for each outage category and voltage level are presented in Table 3.4 where higher values indicate more severe outages. From the table, it is observed that 69 kV is most susceptible to the outage category, Other, followed by Weather and Equipment. For 115 kV, Weather is the most significant category followed by Other and Equipment. For 230 kV, Equipment is the most significant category followed by Other and Human Factors. For 500 kV, the most significant category is External, followed by Other and System Protection.

Table 3.4: Outage classification based on Susceptibility Index (SI)

Outage Category	Outage Cause	69kV	115kV	230kV	500kV
1-Equipment	AC, BK, SU, VA	0.0080	0.0097	0.0764	2.21-05
2- System Protection	CO	0.0003	0.0033	0.0030	0.0050
3- Lines	PO, XF	0.0034	0.0030	0	0
4-Weather	WI, ST	0.0221	0.0542	0.0001	0
5-Lightning	LI	0.0002	0.0025	0	0.0003
6-Unknown	UN, KV,FT	0.0010	0.0007	2.61E-05	2.76E-05
8-External	PC, FS, KV	7.11E-05	0.0047	0.0022	0.2359
9-Other	HU, AN,AU, BI, CN, DE, FI	0.0963	0.0364	0.0603	0.0085
12-Human Factors	IP, SP	3.40E-05	3.45E-05	0.0041	0.0008

While SI is useful in identifying the severity of outage categories specific to a voltage class, it is not useful for comparing outage severity across different years. For example, let us compare SI for 500 kV lines for the years 2009 and 2012 for outage category, External, in Table 3.5. It is observed that although the frequency and duration of outages for the year 2009 was lower than that in 2012, the respective SI values for 2009 (1) and 2012 (0.3929) are not indicative of the severity of the outages in terms of outage duration or frequency. This is because SI which is given by (3.9) is a relative frequency and duration product and it calculates the severity specific to a year, outage category α and voltage class v. It cannot be used for comparing the severity of outages across different years because the severity is not compared with a common base. The base depends on N_v and IT_v which vary according to the year of study and the outage category, and thus SI values for an outage category are not comparable when calculated annually.

Table 3.5: Comparison of Annual Susceptibility Index (SI) for 2009 and 2012

500 kV	2009	2012	2009	2012	2009	2012
	Frequency (#)		Duration (mins)		SI	
1-Equipment	0	0	0	0	0	0
2- System Protection	0	1	0	8	0	0.0002
3- Lines	0	0	0	0	0	0
4-Weather	0	0	0	0	0	0
5-Lightning	0	0	0	0	0	0
6-Unknown	0	0	0	0	0	0
8-External	2	3	214	5778	1	0.3929
9-Other	0	1	0	1543	0	0.0349
12-Human Factors	0	1	0	24	0	0.0005
Total	2	6	214	7353		

3.5.2. Outage Impact Index (OII)

To overcome the shortcomings of SI, a novel index called Outage Impact Index (OII) is proposed in this chapter. OII allows comparison of outage severity in terms of element outage frequency, i.e. the outage frequency for an outage category α and voltage class v, as a fraction of the total elements for the voltage v, and the downtime severity; where downtime is expressed as a fraction of the annual service period. These ratios would serve as a common base for analyzing transmission outage severity according to outage category and voltage class. Thus, this index can be calculated annually and would allow comparison of outage severity across different years. The proposed index, OII, is mathematically defined by

$$OII_{\alpha,v} = \frac{N_{\alpha,v}}{T_v} * \frac{IT_{\alpha,v}}{ET_v} \tag{3.10}$$

where, T_v is the total number of elements for a voltage class v and ET_v is the exposure time for the study period of 1 year (= 8,760 hours). Table 3.6 presents corresponding OII values for the example described in Table 3.5. It is observed from Table 3.6 that OII gives an accurate representation of outage severity for years 2009 (4.52E-05) and 2012 (0.0018)

in contrast to SI values of 1 and 0.39 for the same years (obtained in Table 3.5). We can draw a conclusion from Table 3.6 that outage severity for outage category External is higher for the year 2012 as compared to the year 2009. This index makes it possible to compare severity for each category on an annual basis unlike SI.

Table 3.6: Comparison of Outage Impact Index (OII) for 2009 and 2012

500 kV	2009	2012	2009	2012	2009	2012
	Frequency (#)		Duration (mins)		OII	
1-Equipment	0	0	0	0	0	0
2- System Protection	0	1	0	8	0	8.45E-07
3- Lines	0	0	0	0	0	0
4-Weather	0	0	0	0	0	0
5-Lightning	0	0	0	0	0	0
6-Unknown	0	0	0	0	0	0
8-External	2	3	214	5778	4.52E-05	0.0018
9-Other	0	1	0	1543	0	0.0002
12-Human Factors	0	1	0	24	0	2.52E-06
Total	2	6	214	7353		

Figure 3.12 presents the outage severity based on outage category for the years 2009-2016. It is observed that overall severity for categories: Other (9), Weather (4), External (8), and Equipment (1) are high. Annual investigation of the outage categories would therefore reveal potential risks in terms of both outage downtime and frequency. For example, in Figure 3.13, the annual OII values for the outage category, Other (9), is presented. It is observed that outage severity for this category is in general high with an average value of 0.0004 for 69 kV followed by 115 kV lines. Similarly, all outage categories can be prioritized based on their duration and frequency severity for further investigation. Finally, corrective action such as operation practices, maintenance strategies, and spare management can be developed based on the analysis results. It is important to mention here that identification and prioritization of outages based on frequency and duration as has been done above is not possible with FOHMY.

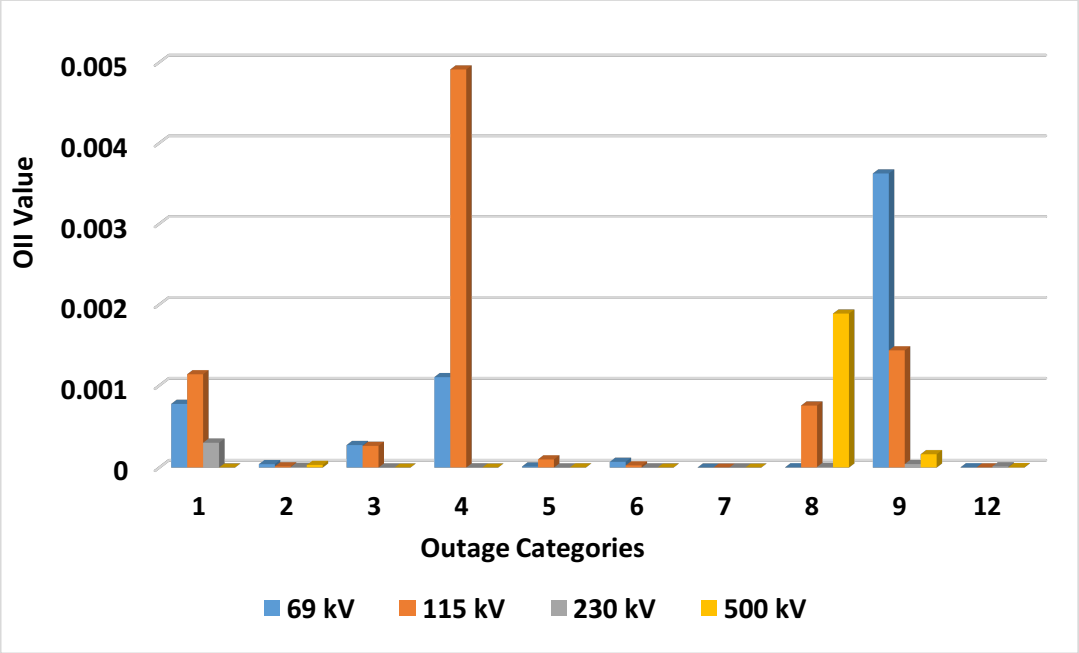

Figure 3.12: Outage Impact Index summary for all outage categories (1-12)

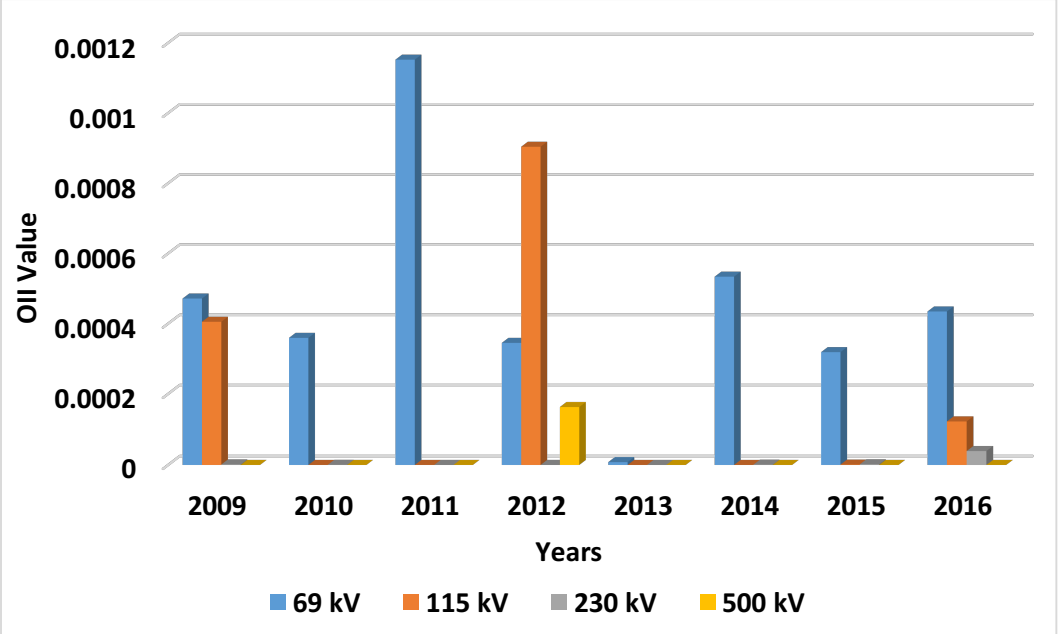

Figure 3.13: Outage Impact Index trend for outage category, Other (9)

3.6. Discussion and Conclusion

Discussion

- The impact of transmission line outages in terms of load lost (MW) can also be incorporated in the definition OII, if that information is available. This can be included in the form of a ratio in terms of the total rated capacity of the line.
- Based on the severity of outages categories identified by OII, further reliability and root-cause analysis may need to be carried out to identify potential system risks and take corrective action.

Conclusion

This chapter has provided a comprehensive summary of the existing methods for computing transmission system reliability through a detailed statistical analysis of historical outage data. These statistics have been instrumental in:

- Establishing chronological outage frequency and duration trends to serve as baselines for future performance assessments
- Calculating the existing transmission network availability based on MTBF and MTTR
- Identifying and prioritizing outage categories through annual outage severity trends

The chapter concludes by presenting a novel transmission reliability index, OII, and shows its effectiveness over FOHMY and SI. The key performance indices discussed here can be used by power utilities to quantify and assess their transmission system performance, establish baselines from chronological trends, and minimize system risks through outage evaluation and development of reliability improvement strategies.

CHAPTER 4

CONCLUSION AND FUTURE SCOPE OF WORK

Reliability of the transmission system is pertinent for ensuring supply of uninterrupted power from generating sources to the end users. A reliable power supply can be maintained by monitoring the power system continuously for disturbances and by quantitatively analyzing failures. One of the major power system disturbances is believed to be uncontrolled islanding. Chapter 2 of this thesis proposes a robust islanding detection technique which is immune to PMU errors and successfully detects islands in the presence of wind energy penetration. Evaluation of power system performance is a crucial step in minimizing reoccurrence of power system disturbances and reducing losses that may be incurred due to these disturbances. This aspect is elaborated in detail in Chapter 3 which emphasizes the importance of analyzing the cause of failures and evaluates system performance to identify potential risks.

The proposed Cumulative Sum of Phase Angle Difference (CUSPAD) islanding detection approach uses PMU voltage phase angle measurements from multiple locations in the network. This approach is able to detect islands efficiently for both 18 bus and 118 bus system with accuracies over 97% at an average. The accuracy of this approach is not affected adversely in the presence of wind energy at various levels of penetration. The accuracy of this approach is also observed to be superior compared to the conventional relative angle difference (AD) of phase angles approach in presence of measurement errors.

The reliability evaluation and outage analysis of failures have established chronological outage frequency and duration trends which would serve as baselines for future performance assessments. Evaluation of the transmission network performance

through calculation of availability using indices such MTBF and MTTR is performed. Further, identification and prioritization of outage categories through annual outage severity trends is carried out. This helped in identification of severe outage categories based on which, corrective action can be planned to prevent recurrence.

Future Scope of Work

During this research work the following scope was identified as future work:

1. Incorporation of frequency in the proposed islanding detection scheme: Effect of inclusion of frequency variations as an additional attribute in the proposed methodology can be studied for improvement in detection accuracy during different base case operating conditions.
2. Modeling protection schemes in the islanding simulations: Reference [6] emphasizes the importance of including protection scheme modeling in dynamic simulations. The performance of islanding detection schemes integrated with protection schemes might provide practical insights on the power system behavior during island formation.
3. Incorporation of Transmission load /MW lost in reliability metric: While MW load lost was not provided in the data made available for this research work, including MW load lost in the formulation of OII would make it possible to access the extent of damage/loss that is caused by a transmission line outage when compared to the nominal line rating.
4. Line fault analysis: Line fault information was also not available in the data used for outage analysis. However, if this information is available, outages can be analyzed further with respect to the type of faults and based on the findings, protection schemes can be augmented, if found necessary.

REFERENCES

[1] D. Ramasubramanian, “Impact of Converter Interfaced Generation and Load on Grid Performance ” PhD. dissertation, Arizona State University, 2017.

[2] K. Verma, S. Ajit, and D. R. Karanki, Reliability and Safety Engineering. Springer, 2016.

[3] D. O. Koval, and A. A. Chowdhury, "Assessment of transmission-line common-mode, station-originated, and fault-type forced-outage rates,” *IEEE Trans. Ind. Appl.*, vol. 46, no. 1, pp. 313-318, Jan.-Feb., 2010.

[4] “Phase Angle Monitoring: Industry Experience Following the 2011 Pacific Southwest Outage Recommendation 27”, NERC, June 2016, [Online] Available: https://www.nerc.com/comm/PC/Synchronized%20Measurement%20Subcommittee/Phase%20Angle%20Monitoring%20Technical%20Reference%20Document%20-%20FINAL.pdf

[5] M. Faifer, M. Khalil, C. Laurano, G. Leone, and S. Toscani, “Outage data analysis and RAMS evaluation of the Italian overhead transmission lines,” in *Proc. IEEE Int. Energy Conf.*, Leuven, Belgium, pp. 1-6, Apr. 4-8, 2016.

[6] M. K. Hedman, “Analytical Approaches for Identification and Representation of Critical Protection Systems in Transient Stability Studies” Ph.D. dissertation, Arizona State University, 2017.

[7] M. B. Selak, “Power System Protection – Where Are We Today?”, December 2015, [Online] Available: http://www.ieee.hr/_download/repository/Selak_-_Power_system_protection_-_Where_are_we_today.pdf

[8] Z. Lin, et al., "Application of wide area measurement systems to islanding detection of bulk power systems" *IEEE Trans. Power Syst.,* vol. 28 no. 2 pp. 2006-2015, 2013.

[9] R. Sun and V. A. Centeno "Wide area system islanding contingency detecting and warning scheme" *IEEE Trans. Power Syst.*, vol. 29 no. 6 pp. 2581-2589 , Nov. 2014.

[10] F Galvan, S Mandal, and M Thomas, “Phasor Measurement Units (PMU) instrumental in detecting and managing the electrical island created in the aftermath of Hurricane Gustav”, *Power Syst. Conf. Expo.*, pp. 1 – 4, Mar 15-18, 2009.

[11] F. Galvan C. H. Wells "Detecting and managing the electrical island created in the aftermath of Hurricane Gustav using Phasor Measurement Units (PMUs)" *in Proc. Transm. Distrib. Conf. Expo*. pp. 1-5, 2010.

[12] S. Kolluri S. Mandal F. Galvan M. Thomas "Island formation in Entergy power grid during Hurricane Gustav" *in Proc. IEEE Power Eng. Soc. Gen. Meeting*. pp. 1-5, July 26–30, 2009.

[13] T. Ohno T. Yasuda O. Takahashi M. Kaminaga S. Imai "Islanding protection system based on synchronized phasor measurements and its operational experiences" in *Proc. IEEE Power Eng. Soc. General Meeting*, pp. 1-5, 2008.

[14] A. Pal, P. Chatterjee, J. S. Thorp, and V. A. Centeno, "On-line calibration of voltage transformers using synchrophasor measurements," *IEEE Trans. Power Del.*, vol. 31, no. 1, pp. 370-380, Feb. 2016.

[15] J. Zhao, et al., "Impact of measurement errors on synchrophasor applications" in *Proc. IEEE Power Eng. Soc. General Meeting*, 2017

[16] S. Wang, E. Farantatos, and K. Tomsovic, "Wind turbine generator modeling considerations for stability studies of weak systems", *North American Power Symposium (NAPS),* 2017

[17] E. E. Bernabeu, J. S. Thorp, and V. A. Centeno, "Methodology for a security/dependability adaptive protection scheme based on data mining," *IEEE Trans. Power Del.*, vol. 27, no. 1, pp. 104-111, Jan. 2012.

[18] M. Doostan and B. H. Chowdhury, "A data-driven analysis of outage duration in power distribution systems," *2017 North American Power Symposium (NAPS)*, Morgantown, WV, 2017, pp. 1-6.

[19] J. Y. Zhang and C. M. Bush, "PMU based islanding detection to improve system operation," in *Proc. IEEE Power Eng. Soc. Gen. Meeting*, Boston, MA, 2016, pp. 1-5, 2016.

[20] H. T. Yip, G. Millar, G. J. Lloyd, A. Dysko, G. M. Burt, and R. Tumilty, "Islanding detection using an accumulated phase angle drift measurement," in *Proc. 10th IET Int .Devel. Power Syst. Protect.,* 2010, pp. 1–5.

[21] A. Ishibashi, et al., "New type of islanding detection system for distributed generation based on voltage angle difference between utility network and distributed generation site", *in Proc IEE Int. Conf. on Develop. in Power Syst.* Prot., pp :542 - 545 , April 2004.

[22] "Using Synchrophasor Data for Phase Angle Monitoring", North American SynchroPhasor Initiative, May 2016. [Online] Available: https://www.naspi.org/sites/default/files/reference_documents/0.pdf

[23] J. D. L. Ree V. Centeno J. S. Thorp A. G. Phadke "Synchronized phasor measurement applications in power systems" *IEEE Trans. on Smart Grid*, vol. 1 no. 1 pp. 20-27 ,June 2010.

[24] F. Aminifar, M. Fotuhi-Firuzabad, A. Safdarian et al., "Synchrophasor measurement technology in power systems: panorama and state-of-the-art", *IEEE Access*, vol. 2, pp. 1607-1628, 2014.

[25] A. Pal, C. Mishra, A. K. S. Vullikanti, and S. S. Ravi, "General optimal substation coverage algorithm for phasor measurement unit placement in practical systems," *IET Gener., Transm. Distrib.*, vol. 11, no. 2, pp. 347-353, Jan. 2017.

[26] C. Mishra, K. D. Jones, A. Pal, and V. A. Centeno, "Binary particle swarm optimisation-based optimal substation coverage algorithm for phasor measurement unit installations in practical systems," *IET Gener. Transm. Distrib.*, vol. 10, no. 2, pp. 555-562, Feb. 2016.

[27] C. Mishra, A. Pal, and V. A. Centeno, "Kalman-filter based recursive regression for three-phase line parameter estimation using phasor measurements," *in Proc. IEEE Power Eng. Soc. General Meeting*, Denver, CO, pp. 1-5, 26-30 Jul. 2015.

[28] J. S. Thorp, A. G. Phadke, S. H. Horowitz, and M. M. Begovic, "Some applications of phasor measurements to adaptive protection," *IEEE Trans. Power Syst.*, vol. 3, no. 2, pp. 791-798, May 1988.

[29] V. A. Centeno, J. De La Ree, A. G. Phadke, G. Michel, R. J. Murphy, and R. O. Burnett, Jr., "Adaptive out-of-step relaying using phasor measurement techniques," *IEEE Comput. Appl. Power*, vol. 6, no. 4, pp. 12-17, Oct. 1993.

[30] T. Wang, A. Pal, J. S. Thorp, Z. Wang, J. Liu, and Y. Yang, "Multi-polytope based adaptive robust damping control in power systems using CART," *IEEE Trans. Power Syst.*, vol. 30, no. 4, pp. 2063-2072, Jul. 2015.

[31] A. Pal, J. S. Thorp, S. S. Veda, and V. A. Centeno, "Applying a robust control technique to damp low frequency oscillations in the WECC*," Int. J. Elect. Power Energy Syst.*, vol. 44, no. 1, pp. 638-645, Jan. 2013.

[32] A. Pal, G. A. Sanchez, V. A. Centeno, and J. S. Thorp, "A PMU placement scheme ensuring real-time monitoring of critical buses of the network," *IEEE Trans. Power Del.,* vol. 29, no. 2, pp. 510-517, Apr. 2014.

[33] Synchrophasor Fact Sheet, North American Synchrophasor Initiative, October 2014 [Online] Available: https://www.naspi.org/sites/default/files/reference_documents/33.pdf?fileID=1326

[34] A. Engelmann, “ComEd Research Interests,” PSERC Summer Workshop, Aug. 2016.

[35] X. Liu, J. Kennedy, D. Laverty, D. J. Morrow and S. McLoone, "Wide area phase angle measurements for islanding detection — An adaptive nonlinear approach," in *Proc. IEEE Power Eng. Soc. General Meeting*, Chicago, IL, 2017, pp. 1-1.

[36] N.W. A. Lidula, and A. D. Rajapakse, “A pattern recognition approach for detecting power islands using transient signals-Part II: performance evaluation,” *IEEE Trans. Power Del.*, vol. 27, no. 3, pp. 1071-1080, Jul. 2012.

[37] N.W. A. Lidula, and A. D. Rajapakse, “A pattern recognition approach for detecting power islands using transient signals-Part I:design and implementation,” *IEEE Trans. Power Del.*, vol. 25, no. 4, pp. 3070-3077, Oct. 2010.

[38] T. Funabashi, K. Koyanagi, and R. Yokoyama, “A review of islanding detection methods for distributed resources,” in *Proc. IEEE Bologna Power Tech Conf.*, vol. 2, pp. 6–11, 2003

[39] P. O’Kane and B. Fox, “Loss of mains detection for embedded generation by system impedance monitoring,” in *Proc. Inst. Elect. Eng. 6th Int. Conf. Develop. Power Syst. Protect.,* pp. 95–98, 1997

[40] W. Freitas, W. Xu, C. M. Affonso, and Z. Haung, “Comparative analysis between ROCOF and vector surge relays for distributed generation applications,” *IEEE Trans. Power Del.*, vol. 20, no. 2, pt. 2, pp.1315–1324, Apr. 2005.

[41] Y. Guo, K. Li, D. M. Laverty, and Y. Xue, “Synchrophasor based island detection for distributed generation systems using systematic principal component analysis,” *IEEE Trans. Power Del.*, vol. 30, no. 6, pp. 2544-2552, Dec. 2015.

[42] A. Yafaoui, B. Wu, and S. Kouro, “Improved active frequency drift antiislanding detection method for grid connected photovoltaic systems,” *IEEE Trans. Power Electron.*, vol. 27, no. 5, pp. 2367-2375, May 2012.

[43] R. Azim, K. Sun, F. Li, Y. Zhu, H. A. Saleem, D. Shi, and R. Sharma,“A comparative analysis of intelligent classifiers for passive island detection in micro-grids,” in *Proc. IEEE Eindhoven PowerTech*, Eindhoven, pp. 1-6, Jul. 2015.

[44] M. R. Alam, K. M. Muttaqi, and A. Bouzerdoum,"A multifeature-based approach for islanding detection of DG in the subcritical region of vector surge relays," *IEEE Trans. Power Del.*, vol. 29, no. 5, pp. 2349-2358, Oct. 2014.

[45] G. Marchesan, M. R. Muraro, G. Cardoso, L. Mariotto, and A. P. deMorais, "Passive method for distributed-generation island detection based on oscillation frequency," *IEEE Trans. Power Del.*, vol. 31, no. 1,pp. 138-146, Feb. 2016.

[46] Y.-H. Liy, T.-S. Luor, S.-J. Huang, and J.-M. Lin, "Method and system for detecting stand-alone operation of a distributed generating system," *U.S. Patent 7 342 758,* Mar. 2008.

[47] C.-T. Hsieh, J.-M. Lin, and S.-J. Huang, "Enhancement of islanding-detection of distributed generation systems via wavelet transform-based approaches," *Int. J. Elect. Power Energy Syst.*, vol.30, no. 10, pp. 575–580, Dec. 2008.

[48] M. A. Redfern, O. Usta, and G. Fielding, "Protection against loss of utility grid supply for a dispersed storage and generation unit," *IEEE Trans. Power Del.,* vol. 8, no. 3, pp. 948–954, Jul. 1993.

[49] X. Liu, D. M. Laverty, R. J. Best, K. Li, D. J. Morrow, and S. S. McLoone, "Principal component analysis of wide-area phasor measurements for islanding detection-a geometric view," *IEEE Trans. Power Del.,* vol. 30, no. 2, pp. 976-985, Apr. 2015.

[50] Laaksonen, H., 'New passive islanding detection method based on the cumulative sum of the change in voltage positive sequence phase angle', *Int.Rev. Model. Simul.*, pp. 1482–1488, 2013.

[51] Y. Liu et al. "Wide-area-measurement system development at the distribution level: An FNET/GridEye example" *IEEE Trans. Power Del.*, vol. 31 no. 2 pp. 721-731 Apr 2016.

[52] "Electricity in the United States," U.S. Energy Information Administration, April 10, 2013, [Online] Available: https://www.eia.gov/energyexplained/

[53] "Wind Energy Facts 101" , AWEA, [Online] Available: https://www.awea.org/windenergyfacts.aspx

[54] “”Western Wind and Solar Integration Study Phase 3 –Frequency Response and Transient Stability: Executive Summary”, NREL, 2014. Online. [Available] https://www.nrel.gov/grid/wwsis.html

[55] Guo, Y. Zhang, M.A. Young et al., "Design and implementation of a real-time off-grid operation detection tool from a wide-area measurements perspective", *IEEE Trans. Smart Grid,* vol. 6, no. 4, pp. 2080-2087, 2015.

[56] S. Nuthalapati, Power system grid operation using synchrophasor technology, Springer International Pu, 2018

[57] M. Rafferty, X. A. Liu, D. Laverty and S. McLoone, "Real-time multiple event detection and classification using moving window PCA," in *Proc. IEEE Power Eng. Soc. General Meeting*, Chicago, IL, 2017, pp. 1-1.

[58] R. Sun, Z. Wu, and V. A. Centeno, “Power system islanding detection & identification using topology approach and decision tree,” *in Proc. IEEE Power Energy Soc. General Meeting*, San Diego, CA, pp. 1-6, 24-29 Jul.2011.

[59] “Wind Power 101”, AWEA, [Online] Available: https://www.awea.org/wind-power-101

[60] T. Ackermann, Wind Power in Power Systems. Wiley, 2012.

[61] R. Bugdal, A. Dysko , G.M. Burt, J McDonald, “Performance analysis of the ROCOF and vector shift methods using a dynamic protection modeling approach” B in *Proc. Int. Conf. on Power Syst. Prot.,* Bled, Slovenia., pp. 139-144, 2006.

[62] IEEE 14 bus system SLD [Online] Available: http://fglongatt.org/OLD/Test_Case_IEEE_14.html

[63] “WECC Wind Power Plant Power Flow Modeling Guide”, WECC Modeling and Validation Work Group, May 2008. [Online] Available: https://www.wecc.biz/Reliability/WECC%20Wind%20Plant%20Power%20Flow%20Modeling%20Guide.pdf

[64] “WECC Wind Plant dynamic modeling guide”, WECC Renewable Energy Modeling Task Force, April 2014, [Online] Available: https://www.wecc.biz/Reliability/WECC%20Wind%20Plant%20Dynamic%20Modeling%20Guidelines.pdf

[65] K Clark, W Miller Nicholas & J Sanchez-Gasca. “Modeling of GE Wind Turbine-Generators for Grid Studies”, GE Energy, 2010

[66] "PSLF," GE Energy Consulting, https://www.geenergyconsulting.com/practice-area/software-products/pslf

[67] Rui Sun, "Wide Area Power System Islanding Detection, Classification and State Evaluation Algorithm", 2012

[68] H. Mori, "State-of-the-art overview on data mining in power systems," in *Proc. IEEE Power Eng. Soc. General Meeting*, 2006.

[69] L. Breiman, J. H. Friedman, R. Olshen, and C. J. Stone, Classification and Regression Tree, Wadsworth & Brooks/Cole Advanced Books & Software, Pacific California, 1984.

[70] M. Asprou, S. Chakrabarti, and E. Kyriakides, "A two-stage state estimator for dynamic monitoring of power systems," *IEEE Syst. J., to be published*, doi: 0.1109/JSYST.2014.2375951.

[71] Asprou, M. and Kyriakides, E. " Identification and Estimation of Erroneous Transmission Line Parameters Using PMU Measurements:, *IEEE Trans. on Power Del.*, pp.1-1, 2017

[72] F. Gao, J. S. Thorp, A. Pal, and S. Gao, "Dynamic state prediction based on Auto-Regressive (AR) model using PMU data," in *Proc. IEEE Power Energy Conf. Illinois (PECI),* Champaign, IL, pp. 1-5, 24-25 Feb. 2012.

[73] A Pal, "PMU-Based Applications for Improved Monitoring and Protection of Power Systems" PhD. dissertation, Polytechnic Institute and StateUniversity, 2014

[74] A. Pal, A. K. S. Vullikanti, and S. S. Ravi, "A PMU placement scheme considering realistic costs and modern trends in relaying," *IEEE Trans. Power Syst.*, vol. 32, no. 1, pp. 552-561, Jan. 2017.

[75] S. Garlapati, & J. Thorp , Choice of reference in CART applications using PMU data, 2011

[76] R. Billinton, and R. Allan, Reliability Evaluation of Engineering Systems: Concepts and Techniques, New York : Springer Science, 1992.

[77] Special Reliability Assessment, NERC, 2017 [Online]. Available: https://www.nerc.com/pa/RAPA/ra/Reliability%20Assessments%20DL/NERC_SPOD_11142017_Final.pdf

[78] “Reliability of Electric Utility Distribution Systems: EPRI White Paper”, EPRI, October 2000 [Online]. Available: http://www.ecosync.com/tdworld/EPRI1000424.pdf

[79] J. Endrenyi, Reliability Modelling in Electric Power System, New York : Wiley, 1978.

[80] Distribution System Reliability Indices [Online]: http://www.mahadiscom.com/emagazine/mar06/what%20are%20saifi.shtm

[81] IEEE Standard Terms for Reporting and Analyzing Outage Occurrences and Outage States of Electrical Transmission Facilities, IEEE Std. 859-1987.

[82] IEEE Recommended Practice for the Design of Reliable Industrial and Commercial Power Systems, IEEE Std. 493-2007.

[83] “Transmission Availability Data System (TADS) Final Phase I (Automatic Outages) Report”, NERC, 2007 [Online] Available: https://www.nerc.com/pa/RAPA/tads/TransmissionAvailabilityDataSyatemRF/TADS_PC_Revised_Final_Report_09_26_07.pdf

[84] M. Papic et al., "Transmission availability data system (TADS) reporting and data analysis," in Proc. IEEE Int. Conf. Probabilistic Methods Applied to Power Syst. (PMAPS 2016), Beijing, China, pp. 1-7, Oct.16-20 2016.

[85] M. Papic, J. J. Bian, and S. Ekisheva, "A novel statistical-based analysis of WECC bulk transmission reliability data," in Proc. IEEE Power Eng. Soc. Gen. Meeting, Vancouver, BC, Canada, pp. 1-5, Jul. 21-25, 2013.

APPENDIX A

DYNAMIC DATA OF TYPE IV WIND TURBINES

The dynamic data of the Type IV wind turbine generator in GE PSLF software is given as follows:

- wt4g Bus no. "Bus name" 0.6 "1 " : #9 MVA 1.0000 10.000 0.9000/ 0.4000 1.2200 1.2000 0.8000 0.4000 -1.300 0.7000
- wt4e Bus no. "Bus name" 0.6 "1 " : #9 1.0000 0.1000 20.00 1.1000 / 0.900 4000 -0.4000 0.0200 0.150 18.000 5.000 1.0000 0.0500 0.0500 1.2400 / 0.901 1.2500 0.0000 1.700 1.600
- wt4t Bus no. "Bus name" 0.6 "1 " : #9 0.0500 0.0800 0.1000 0.0800 / 0.000 0.1000 -0.1000

Controller gains for wind turbine models are as below:

- Controller gains for Wt4g:

  Kpp 0.08 PI controller proportional gain, p.u.

  Kip 0.10 PI controller integral gain, p.u

- Controller gains for Wt4e:

  Kqi 0.1 Q control integral gain

  Kvi 12. V control integral gain

APPENDIX B

MODIFIED 118 BUS SYSTEM DATA WITH 10% WIND PENETRATION

Bus data

Bus	Type	V (p.u.)	V(deg.)	Bus	Type	V (p.u.)	V(deg.)
1	2	0.9705	-17.31	37	1	0.9919	-16.21
2	1	0.9773	-16.64	38	1	0.9619	-11.05
3	1	0.979	-16.37	39	1	0.9704	-19.59
4	2	1.01	-12.7	40	2	0.97	-20.67
5	1	1.0101	-12.21	41	1	0.9668	-21.12
6	2	0.99	-14.79	42	2	0.985	-19.54
7	1	0.9893	-15.23	43	1	0.9785	-16.73
8	2	1.015	-7.2	44	1	0.985	-14.27
9	1	1.0049	0.49	45	1	0.9867	-12.45
10	2	0.9763	9.11	46	2	1.005	-9.65
11	1	0.9887	-15.12	47	1	1.017	-7.43
12	2	0.99	-15.58	48	1	1.0206	-8.21
13	1	0.9711	-16.5	49	2	1.025	-7.21
14	1	0.9836	-16.32	50	1	1.0213	-9.54
15	2	0.97	-16.69	51	1	1.0153	-12.44
16	1	0.9839	-15.92	52	1	1.0137	-13.46
17	1	0.9951	-14.19	53	1	1.0253	-14.6
18	2	0.973	-16.4	54	2	1.049	-14.01
19	2	0.9631	-16.88	55	2	1.0346	-14.09
20	1	0.956	-16.04	56	2	1.0368	-13.95
21	1	0.9553	-14.47	57	1	1.0273	-12.48
22	1	0.965	-11.93	58	1	1.0223	-13.36
23	1	0.9927	-7	59	2	0.9862	-8.79
24	2	0.992	-7.24	60	1	0.9932	-4.97
25	2	1.027	0.23	61	2	0.995	-4.07
26	2	1.015	1.97	62	2	0.998	-4.7
27	2	0.968	-12.77	63	1	0.9692	-5.37
28	1	0.9616	-14.46	64	1	0.9839	-3.58
29	1	0.9632	-15.43	65	2	1.005	-0.38
30	1	0.9854	-9.13	66	2	1.039	-0.51
31	2	0.967	-15.3	67	1	1.0137	-3.23
32	2	0.963	-13.28	68	1	1.0005	-0.47
33	1	0.9715	-17.31	69	0	1.035	1.8
34	2	0.9858	-16.67	70	2	1.0115	-5.94
35	1	0.9807	-17.1	71	1	1.0008	-6.16
36	2	0.98	-17.09	72	2	0.98	-7.14

Bus	Type	V (p.u.)	V(deg.)	Bus	Type	V (p.u.)	V(deg.)
73	2	0.991	-6.22	113	2	0.993	-14.21
74	2	1.0322	-7.65	114	1	0.9601	-13.63
75	1	1.0072	-5.96	115	1	0.96	-13.64
76	2	0.9701	-6.95	116	2	1.005	-0.92
77	2	0.9853	-1.46	117	1	0.9738	-17.12
78	1	0.9783	-1.71	118	1	0.9836	-6.85
79	1	0.9757	-1.29				
80	1	0.9841	1.44				
280	1	0.9841	14.75				
380	2	1.04	27.34				
81	1	0.9749	0.31				
82	1	0.9709	-0.93				
83	1	0.972	0.21				
84	1	0.9757	2.63				
85	2	0.985	4.11				
86	1	0.9867	2.74				
87	2	1.015	3				
88	1	0.9874	7.25				
89	2	1.005	11.32				
90	2	0.985	4.91				
91	2	0.98	4.92				
92	2	0.99	5.46				
93	1	0.9803	2.51				
94	1	0.9802	0.4				
95	1	0.9647	-0.5				
96	1	0.9696	-0.54				
97	1	0.9719	0.05				
98	1	0.988	-0.55				
99	2	1.01	-1.35				
100	2	1.017	-0.38				
101	1	0.9914	1.22				
102	1	0.9891	3.94				
103	2	1.0007	-3.97				
104	2	0.971	-6.72				
105	2	0.966	-7.84				
106	1	0.9618	-8.09				
107	2	0.952	-10.88				
108	1	0.9668	-9.03				
109	1	0.9675	-9.48				
110	2	0.973	-10.32				
111	2	0.98	-8.67				
112	2	0.975	-13.42				

Line Data

From	To	R(p.u.)	X(p.u.)	B(p.u.)
1	2	0.0303	0.0999	0.0254
1	3	0.0129	0.0424	0.0108
2	12	0.0187	0.0616	0.0157
3	5	0.0241	0.108	0.0284
3	12	0.0484	0.16	0.0406
4	5	0.0018	0.008	0.0021
4	11	0.0209	0.0688	0.0175
5	6	0.0119	0.054	0.0143
5	11	0.0203	0.0682	0.0174
6	7	0.0046	0.0208	0.0055
7	12	0.0086	0.034	0.0087
8	9	0.0024	0.0305	1.162
8	30	0.0043	0.0504	0.514
9	10	0.0026	0.0322	1.23
11	12	0.006	0.0196	0.005
11	13	0.0223	0.0731	0.0188
12	14	0.0215	0.0707	0.0182
12	16	0.0212	0.0834	0.0214
12	117	0.0329	0.14	0.0358
13	15	0.0744	0.2444	0.0627
14	15	0.0595	0.195	0.0502
15	17	0.0132	0.0437	0.0444
15	19	0.012	0.0394	0.0101
15	33	0.038	0.1244	0.0319
16	17	0.0454	0.1801	0.0466
17	18	0.0123	0.0505	0.013
17	31	0.0474	0.1563	0.0399
17	113	0.0091	0.0301	0.0077
18	19	0.0112	0.0493	0.0114
19	20	0.0252	0.117	0.0298
19	34	0.0752	0.247	0.0632
20	21	0.0183	0.0849	0.0216
21	22	0.0209	0.097	0.0246
22	23	0.0342	0.159	0.0404
23	24	0.0135	0.0492	0.0498
23	25	0.0156	0.08	0.0864
23	32	0.0317	0.1153	0.1173
24	70	0.0022	0.4115	0.102
24	72	0.0488	0.196	0.0488
25	27	0.0318	0.163	0.1764

From	To	R(p.u.)	X(p.u.)	B(p.u.)
26	30	0.008	0.086	0.908
27	28	0.0191	0.0855	0.0216
27	32	0.0229	0.0755	0.0193
27	115	0.0164	0.0741	0.0197
28	29	0.0237	0.0943	0.0238
29	31	0.0108	0.0331	0.0083
30	38	0.0046	0.054	0.422
31	32	0.0298	0.0985	0.0251
32	113	0.0615	0.203	0.0518
32	114	0.0135	0.0612	0.0163
33	37	0.0415	0.142	0.0366
34	36	0.0087	0.0268	0.0057
34	37	0.0026	0.0094	0.0098
34	43	0.0413	0.1681	0.0423
35	36	0.0022	0.0102	0.0027
35	37	0.011	0.0497	0.0132
37	39	0.0321	0.106	0.027
37	40	0.0593	0.168	0.042
38	65	0.009	0.0986	1.046
39	40	0.0184	0.0605	0.0155
40	41	0.0145	0.0487	0.0122
40	42	0.0555	0.183	0.0466
41	42	0.041	0.135	0.0344
42	49	0.0715	0.323	0.086
42	49	0.0715	0.323	0.086
43	44	0.0608	0.2454	0.0607
44	45	0.0224	0.0901	0.0224
45	46	0.04	0.1356	0.0332
45	49	0.0684	0.186	0.0444
46	47	0.038	0.127	0.0316
46	48	0.0601	0.189	0.0472
47	49	0.0191	0.0625	0.016
47	69	0.0844	0.2778	0.0709
48	49	0.0179	0.0505	0.0126
49	50	0.0267	0.0752	0.0187
49	51	0.0486	0.137	0.0342
49	54	0.0869	0.291	0.073
49	54	0.073	0.289	0.0738
49	66	0.018	0.0919	0.0248
49	66	0.018	0.0919	0.0248

From	To	R(p.u.)	X(p.u.)	B(p.u.)
49	69	0.0985	0.324	0.0828
50	57	0.0474	0.134	0.0332
51	52	0.0203	0.0588	0.014
51	58	0.0255	0.0719	0.0179
52	53	0.0405	0.1635	0.0406
53	54	0.0263	0.122	0.031
54	55	0.0169	0.0707	0.0202
54	56	0.0027	0.0095	0.0073
54	59	0.0503	0.2293	0.0598
55	56	0.0049	0.0151	0.0037
55	59	0.0474	0.2158	0.0565
56	57	0.0343	0.0966	0.0242
56	58	0.0343	0.0966	0.0242
56	59	0.0803	0.239	0.0536
56	59	0.0825	0.251	0.0569
59	60	0.0317	0.145	0.0376
59	61	0.0328	0.15	0.0388
60	61	0.0026	0.0135	0.0146
60	62	0.0123	0.0561	0.0147
61	62	0.0082	0.0376	0.0098
62	66	0.0482	0.218	0.0578
62	67	0.0258	0.117	0.031
63	64	0.0017	0.02	0.216
64	65	0.0027	0.0302	0.38
65	68	0.0014	0.016	0.638
66	67	0.0224	0.1015	0.0268
68	81	0.0018	0.0202	0.808
68	116	0.0003	0.0041	0.164
69	70	0.03	0.127	0.122
69	75	0.0405	0.122	0.124
69	77	0.0309	0.101	0.1038
70	71	0.0088	0.0355	0.0088
70	74	0.0401	0.1323	0.0337
70	75	0.0428	0.141	0.036
71	72	0.0446	0.18	0.0444
71	73	0.0087	0.0454	0.0118
74	75	0.0123	0.0406	0.0103
75	77	0.0601	0.1999	0.0498
75	118	0.0145	0.0481	0.012
76	77	0.0444	0.148	0.0368
76	118	0.0164	0.0544	0.0136
77	78	0.0038	0.0124	0.0126
77	80	0.0294	0.105	0.0228

From	To	R(p.u.)	X(p.u.)	B(p.u.)
77	80	0.017	0.0485	0.0472
77	82	0.0298	0.0853	0.0817
78	79	0.0055	0.0244	0.0065
79	80	0.0156	0.0704	0.0187
80	96	0.0356	0.182	0.0494
80	97	0.0183	0.0934	0.0254
80	98	0.0238	0.108	0.0286
80	99	0.0454	0.206	0.0546
82	83	0.0112	0.0366	0.038
82	96	0.0162	0.053	0.0544
83	84	0.0625	0.132	0.0258
83	85	0.043	0.148	0.0348
84	85	0.0302	0.0641	0.0123
85	86	0.035	0.123	0.0276
85	88	0.02	0.102	0.0276
85	89	0.0239	0.173	0.047
86	87	0.0283	0.2074	0.0445
88	89	0.0139	0.0712	0.0193
89	90	0.0518	0.188	0.0528
89	90	0.0238	0.0997	0.106
89	92	0.0393	0.1581	0.0414
89	92	0.0099	0.0505	0.0548
90	91	0.0254	0.0836	0.0214
91	92	0.0387	0.1272	0.0327
92	93	0.0258	0.0848	0.0218
92	94	0.0481	0.158	0.0406
92	100	0.0648	0.295	0.0472
92	102	0.0123	0.0559	0.0146
93	94	0.0223	0.0732	0.0188
94	95	0.0132	0.0434	0.0111
94	96	0.0269	0.0869	0.023
94	100	0.0178	0.058	0.0604
95	96	0.0171	0.0547	0.0147
96	97	0.0173	0.0885	0.024
98	100	0.0397	0.179	0.0476
99	100	0.018	0.0813	0.0216
100	101	0.0277	0.1262	0.0328
100	103	0.016	0.0525	0.0536
100	104	0.0451	0.204	0.0541
100	106	0.0605	0.229	0.062
101	102	0.0246	0.112	0.0294
103	104	0.0466	0.1584	0.0407
103	105	0.0535	0.1625	0.0408

From	To	R(p.u.)	X(p.u.)	B(p.u.)
103	110	0.0391	0.1813	0.0461
104	105	0.0099	0.0378	0.0099
105	106	0.014	0.0547	0.0143
105	107	0.053	0.183	0.0472
105	108	0.0261	0.0703	0.0184
106	107	0.053	0.183	0.0472
108	109	0.0105	0.0288	0.0076
109	110	0.0278	0.0762	0.0202
110	111	0.022	0.0755	0.02
110	112	0.0247	0.064	0.062
114	115	0.0023	0.0104	0.0028

Transformer Data

From	To	MVA	R(p.u.)	X(p.u.)
8	5	100	0	0.0267
26	25	100	0	0.0382
30	17	100	0	0.0388
38	37	100	0	0.0375
63	59	100	0	0.0386
64	61	100	0	0.0268
65	66	100	0	0.037
68	69	100	0	0.037
81	80	100	0	0.037
80	280	100	0	0.05
280	380	100	0	0.05

Generator Data

Bus	Pg(MW)	Qg(MVar)	Bus	Pg(MW)	Qg(MVar)
1	0	15	36	0	-1.1
4	0	46.4	40	0	27
6	0	0.9	42	0	41
8	0	160.6	46	19	-5.2
10	450	-147	49	204	13.8
12	85	56.8	54	48	262.8
15	0	2.7	55	0	23
18	0	26.2	56	0	-8
19	0	-8	59	155	-60
24	0	-7.8	61	160	-42.6
25	220	-47	62	0	11.3
26	314	74.1	65	391	130
27	0	18.4	66	392	-67
31	7	32.6	69	518.2	-110.4
32	0	-10.5	70	0	32
34	0	-8	72	0	-18.7

Bus	Pg(MW)	Qg(MVar)
73	0	-20.8
74	0	9
76	0	23
77	0	70
380	477	26.6
85	0	8.4
87	4	11
89	607	-5.9
90	0	59.3
91	0	-13.1
92	0	-2.1
99	0	10.2
100	252	150
103	40	40
104	0	5.7
105	0	-8
107	0	5.7
110	0	4.9
111	36	-1.8
112	0	41.5
113	0	6.6
116	0	120.8

Shunt Data

Bus	G(pu)	B(pu)
5	0	-0.4
34	0	0.14
37	0	-0.25
44	0	0.1
45	0	0.1
46	0	0.1
48	0	0.15
74	0	1.1
79	0	0.2
82	0	0.2
83	0	0.1
105	0	0.2
107	0	0.06
110	0	0.06

Load Data

Bus	Pload	Qload	Bus	Pload	Qload	Bus	Pload	Qload
1	51	27	49	87	30	99	42	0
2	20	9	50	17	4	100	37	18
3	39	10	51	17	8	101	22	15
4	39	12	52	18	5	102	5	3
6	52	22	53	23	11	103	23	16
7	19	2	54	113	32	104	38	25
8	28	0	55	63	22	105	31	26
11	70	23	56	84	18	106	43	16
12	47	10	57	12	3	107	50	12
13	34	16	58	12	3	108	2	1
14	14	1	59	277	113	109	8	3
15	90	30	60	78	3	110	39	30
16	25	10	62	77	14	112	68	13
17	11	3	66	39	18	113	6	0
18	60	34	67	28	7	114	8	3
19	45	25	70	66	20	115	22	7
20	18	3	72	12	0	116	184	0
21	14	8	73	6	0	117	20	8
22	10	5	74	68	27	118	33	15
23	7	3	75	47	11			
24	13	0	76	68	36			
27	71	13	77	61	28			
28	17	7	78	71	26			
29	24	4	79	39	32			
31	43	27	80	130	26			
32	59	23	82	54	27			
33	23	9	83	20	10			
34	59	26	84	11	7			
35	33	9	85	24	15			
36	31	17	86	21	10			
39	27	11	88	48	10			
40	66	23	90	163	42			
41	37	10	91	10	0			
42	96	23	92	65	10			
43	18	7	93	12	7			
44	16	8	94	30	16			
45	53	22	95	42	31			
46	28	10	96	38	15			
47	34	0	97	15	9			
48	20	11	98	34	8			

APPENDIX C
MODIFIED 118 BUS SYSTEM DATA WITH 20% WIND PENETRATION

Bus data

Bus	Type	V (p.u.)	V(deg.)	Bus	Type	V (p.u.)	V(deg.)
1	2	0.9561	-17.3	35	1	0.9807	-17.2
2	1	0.9587	-16.53	36	2	0.98	-17.2
3	1	0.9666	-16.36	37	1	0.9919	-16.31
4	2	1.01	-12.8	38	1	0.9617	-11.14
5	1	1.0086	-12.29	39	1	0.9704	-19.71
6	2	0.99	-14.89	40	2	0.97	-20.8
7	1	0.9814	-15.22	41	1	0.9668	-21.26
8	2	1.015	-7.28	42	2	0.985	-19.69
9	1	1.0049	0.41	43	1	0.9785	-16.86
10	2	0.9763	9.04	44	1	0.9851	-14.44
11	1	0.9756	-15.04	45	1	0.9867	-12.63
12	1	0.9691	-15.38	46	2	1.005	-9.83
212	1	1.0166	-13.07	47	1	1.017	-7.6
312	2	1.0702	-10.97	48	1	1.0206	-8.41
13	1	0.9608	-16.49	49	2	1.025	-7.42
14	1	0.9681	-16.23	50	1	1.0208	-9.79
15	2	0.97	-16.81	51	1	1.0145	-12.75
16	1	0.9692	-15.83	52	1	1.013	-13.78
17	1	0.9943	-14.28	53	1	1.025	-14.97
18	2	0.973	-16.51	54	2	1.049	-14.41
19	2	0.9631	-17	55	2	1.0321	-14.46
20	1	0.956	-16.15	56	2	1.035	-14.33
21	1	0.9553	-14.57	57	1	1.026	-12.81
22	1	0.9649	-12.02	58	1	1.0211	-13.7
23	1	0.9927	-7.08	59	1	0.966	-8.91
24	2	0.992	-7.31	259	1	0.9981	-4.6
25	2	1.027	0.15	359	2	1.04	-0.6
26	2	1.015	1.89	60	1	0.9651	-4.93
27	2	0.968	-12.86	61	1	0.965	-3.97
28	1	0.9616	-14.56	261	1	0.9748	0.59
29	1	0.9632	-15.52	361	2	0.995	5.02
30	1	0.9851	-9.21	62	2	0.9747	-4.7
31	2	0.967	-15.39	63	1	0.9515	-5.36
32	2	0.963	-13.37	64	1	0.9673	-3.51
33	1	0.9715	-17.43	65	2	1.005	-0.41
34	2	0.9858	-16.77	66	2	1.0354	-0.6

Bus	Type	V (p.u.)	V(deg.)	Bus	Type	V (p.u.)	V(deg.)
67	1	1.0008	-3.28	101	1	0.9914	1.21
68	1	1.0005	-0.48	102	1	0.9891	3.93
69	0	1.035	1.8	103	2	1.0007	-3.98
70	2	1.0115	-5.95	104	2	0.971	-6.73
71	1	1.0008	-6.18	105	2	0.966	-7.85
72	2	0.98	-7.18	106	1	0.9618	-8.1
73	2	0.991	-6.24	107	2	0.952	-10.89
74	2	1.0321	-7.66	108	1	0.9668	-9.04
75	1	1.0072	-5.97	109	1	0.9675	-9.49
76	2	0.9701	-6.96	110	2	0.973	-10.33
77	2	0.9853	-1.47	111	2	0.98	-8.68
78	1	0.9783	-1.71	112	2	0.975	-13.43
79	1	0.9757	-1.3	113	2	0.993	-14.32
80	1	0.984	1.43	114	1	0.9601	-13.72
280	1	0.9841	14.74	115	1	0.96	-13.73
380	2	1.04	27.33	116	2	1.005	-0.93
81	1	0.9749	0.3	117	1	0.9524	-16.99
82	1	0.9709	-0.94	118	1	0.9836	-6.86
83	1	0.972	0.2				
84	1	0.9757	2.62				
85	2	0.985	4.1				
86	1	0.9867	2.73				
87	2	1.015	2.99				
88	1	0.9874	7.24				
89	2	1.005	11.31				
90	2	0.985	4.9				
91	2	0.98	4.91				
92	2	0.99	5.45				
93	1	0.9803	2.5				
94	1	0.9802	0.39				
95	1	0.9647	-0.51				
96	1	0.9695	-0.55				
97	1	0.9719	0.04				
98	1	0.988	-0.56				
99	2	1.01	-1.37				
100	2	1.017	-0.39				

Line Data

From	To	R(p.u.)	X(p.u.)	B(p.u.)
1	2	0.0303	0.0999	0.0254
1	3	0.0129	0.0424	0.0108
2	12	0.0187	0.0616	0.0157
3	5	0.0241	0.108	0.0284
3	12	0.0484	0.16	0.0406
4	5	0.0018	0.008	0.0021
4	11	0.0209	0.0688	0.0175
5	6	0.0119	0.054	0.0143
5	11	0.0203	0.0682	0.0174
6	7	0.0046	0.0208	0.0055
7	12	0.0086	0.034	0.0087
8	9	0.0024	0.0305	1.162
8	30	0.0043	0.0504	0.514
9	10	0.0026	0.0322	1.23
11	12	0.006	0.0196	0.005
11	13	0.0223	0.0731	0.0188
12	14	0.0215	0.0707	0.0182
12	16	0.0212	0.0834	0.0214
12	117	0.0329	0.14	0.0358
13	15	0.0744	0.2444	0.0627
14	15	0.0595	0.195	0.0502
15	17	0.0132	0.0437	0.0444
15	19	0.012	0.0394	0.0101
15	33	0.038	0.1244	0.0319
16	17	0.0454	0.1801	0.0466
17	18	0.0123	0.0505	0.013
17	31	0.0474	0.1563	0.0399
17	113	0.0091	0.0301	0.0077
18	19	0.0112	0.0493	0.0114
19	20	0.0252	0.117	0.0298
19	34	0.0752	0.247	0.0632
20	21	0.0183	0.0849	0.0216
21	22	0.0209	0.097	0.0246
22	23	0.0342	0.159	0.0404
23	24	0.0135	0.0492	0.0498
23	25	0.0156	0.08	0.0864
23	32	0.0317	0.1153	0.1173
24	70	0.0022	0.4115	0.102
24	72	0.0488	0.196	0.0488
25	27	0.0318	0.163	0.1764

From	To	R(p.u.)	X(p.u.)	B(p.u.)
26	30	0.008	0.086	0.908
27	28	0.0191	0.0855	0.0216
27	32	0.0229	0.0755	0.0193
27	115	0.0164	0.0741	0.0197
28	29	0.0237	0.0943	0.0238
29	31	0.0108	0.0331	0.0083
30	38	0.0046	0.054	0.422
31	32	0.0298	0.0985	0.0251
32	113	0.0615	0.203	0.0518
32	114	0.0135	0.0612	0.0163
33	37	0.0415	0.142	0.0366
34	36	0.0087	0.0268	0.0057
34	37	0.0026	0.0094	0.0098
34	43	0.0413	0.1681	0.0423
35	36	0.0022	0.0102	0.0027
35	37	0.011	0.0497	0.0132
37	39	0.0321	0.106	0.027
37	40	0.0593	0.168	0.042
38	65	0.009	0.0986	1.046
39	40	0.0184	0.0605	0.0155
40	41	0.0145	0.0487	0.0122
40	42	0.0555	0.183	0.0466
41	42	0.041	0.135	0.0344
42	49	0.0715	0.323	0.086
42	49	0.0715	0.323	0.086
43	44	0.0608	0.2454	0.0607
44	45	0.0224	0.0901	0.0224
45	46	0.04	0.1356	0.0332
45	49	0.0684	0.186	0.0444
46	47	0.038	0.127	0.0316
46	48	0.0601	0.189	0.0472
47	49	0.0191	0.0625	0.016
47	69	0.0844	0.2778	0.0709
48	49	0.0179	0.0505	0.0126
49	50	0.0267	0.0752	0.0187
49	51	0.0486	0.137	0.0342
49	54	0.0869	0.291	0.073
49	54	0.073	0.289	0.0738
49	66	0.018	0.0919	0.0248
49	66	0.018	0.0919	0.0248

From	To	R(p.u.)	X(p.u.)	B(p.u.)
49	69	0.0985	0.324	0.0828
50	57	0.0474	0.134	0.0332
51	52	0.0203	0.0588	0.014
51	58	0.0255	0.0719	0.0179
52	53	0.0405	0.1635	0.0406
53	54	0.0263	0.122	0.031
54	55	0.0169	0.0707	0.0202
54	56	0.0027	0.0095	0.0073
54	59	0.0503	0.2293	0.0598
55	56	0.0049	0.0151	0.0037
55	59	0.0474	0.2158	0.0565
56	57	0.0343	0.0966	0.0242
56	58	0.0343	0.0966	0.0242
56	59	0.0803	0.239	0.0536
56	59	0.0825	0.251	0.0569
59	60	0.0317	0.145	0.0376
59	61	0.0328	0.15	0.0388
60	61	0.0026	0.0135	0.0146
60	62	0.0123	0.0561	0.0147
61	62	0.0082	0.0376	0.0098
62	66	0.0482	0.218	0.0578
62	67	0.0258	0.117	0.031
63	64	0.0017	0.02	0.216
64	65	0.0027	0.0302	0.38
65	68	0.0014	0.016	0.638
66	67	0.0224	0.1015	0.0268
68	81	0.0018	0.0202	0.808
68	116	0.0003	0.0041	0.164
69	70	0.03	0.127	0.122
69	75	0.0405	0.122	0.124
69	77	0.0309	0.101	0.1038
70	71	0.0088	0.0355	0.0088
70	74	0.0401	0.1323	0.0337
70	75	0.0428	0.141	0.036
71	72	0.0446	0.18	0.0444
71	73	0.0087	0.0454	0.0118
74	75	0.0123	0.0406	0.0103
75	77	0.0601	0.1999	0.0498
75	118	0.0145	0.0481	0.012
76	77	0.0444	0.148	0.0368
76	118	0.0164	0.0544	0.0136
77	78	0.0038	0.0124	0.0126
77	80	0.0294	0.105	0.0228
77	80	0.017	0.0485	0.0472

From	To	R(p.u.)	X(p.u.)	B(p.u.)
77	82	0.0298	0.0853	0.0817
78	79	0.0055	0.0244	0.0065
79	80	0.0156	0.0704	0.0187
80	96	0.0356	0.182	0.0494
80	97	0.0183	0.0934	0.0254
80	98	0.0238	0.108	0.0286
80	99	0.0454	0.206	0.0546
82	83	0.0112	0.0366	0.038
82	96	0.0162	0.053	0.0544
83	84	0.0625	0.132	0.0258
83	85	0.043	0.148	0.0348
84	85	0.0302	0.0641	0.0123
85	86	0.035	0.123	0.0276
85	88	0.02	0.102	0.0276
85	89	0.0239	0.173	0.047
86	87	0.0283	0.2074	0.0445
88	89	0.0139	0.0712	0.0193
89	90	0.0518	0.188	0.0528
89	90	0.0238	0.0997	0.106
89	92	0.0393	0.1581	0.0414
89	92	0.0099	0.0505	0.0548
90	91	0.0254	0.0836	0.0214
91	92	0.0387	0.1272	0.0327
92	93	0.0258	0.0848	0.0218
92	94	0.0481	0.158	0.0406
92	100	0.0648	0.295	0.0472
92	102	0.0123	0.0559	0.0146
93	94	0.0223	0.0732	0.0188
94	95	0.0132	0.0434	0.0111
94	96	0.0269	0.0869	0.023
94	100	0.0178	0.058	0.0604
95	96	0.0171	0.0547	0.0147
96	97	0.0173	0.0885	0.024
98	100	0.0397	0.179	0.0476
99	100	0.018	0.0813	0.0216
100	101	0.0277	0.1262	0.0328
100	103	0.016	0.0525	0.0536
100	104	0.0451	0.204	0.0541
100	106	0.0605	0.229	0.062
101	102	0.0246	0.112	0.0294
103	104	0.0466	0.1584	0.0407
103	105	0.0535	0.1625	0.0408
103	110	0.0391	0.1813	0.0461
104	105	0.0099	0.0378	0.0099

From	To	R(p.u.)	X(p.u.)	B(p.u.)
105	106	0.014	0.0547	0.0143
105	107	0.053	0.183	0.0472
105	108	0.0261	0.0703	0.0184
106	107	0.053	0.183	0.0472
108	109	0.0105	0.0288	0.0076
109	110	0.0278	0.0762	0.0202
110	111	0.022	0.0755	0.02
110	112	0.0247	0.064	0.062
114	115	0.0023	0.0104	0.0028

Transformer Data

From	To	MVA	R(p.u.)	X(p.u.)
8	5	100	0	0.0267
26	25	100	0	0.0382
30	17	100	0	0.0388
38	37	100	0	0.0375
63	59	100	0	0.0386
64	61	100	0	0.0268
65	66	100	0	0.037
68	69	100	0	0.037
81	80	100	0	0.037
12	212	100	0	0.05
59	259	100	0	0.05
61	261	100	0	0.05
80	280	100	0	0.05
212	312	100	0	0.05
259	359	100	0	0.05
261	361	100	0	0.05
280	380	100	0	0.05

Generator Data

Bus	Pg(MW)	Qg(MVar)	Bus	Pg(MW)	Qg(MVar)
1	0	15	65	391	130
4	0	46.4	66	392	-67
6	0	0.9	69	518.2	-110.4
8	0	160.6	70	0	32
10	450	-147	72	0	-18.7
12	85	56.8	73	0	-20.8
15	0	2.7	74	0	9
18	0	26.2	76	0	23
19	0	-8	77	0	70
24	0	-7.8	380	477	26.6
25	220	-47	85	0	8.4

Bus	Pg(MW)	Qg(MVar)	Bus	Pg(MW)	Qg(MVar)
27	0	18.4	89	607	-5.9
31	7	32.6	90	0	59.3
32	0	-10.5	91	0	-13.1
34	0	-8	92	0	-2.1
36	0	-1.1	99	0	10.2
40	0	27	100	252	150
42	0	41	103	40	40
46	19	-5.2	104	0	5.7
49	204	13.8	105	0	-8
54	48	262.8	107	0	5.7
55	0	23	110	0	4.9
56	0	-8	111	36	-1.8
59	155	-60	112	0	41.5
61	160	-42.6	113	0	6.6
62	0	11.3	116	0	120.8

Load Data

Bus	Pload	Qload	Bus	Pload	Qload	Bus	Pload	Qload
1	51	27	49	87	30	99	42	0
2	20	9	50	17	4	100	37	18
3	39	10	51	17	8	101	22	15
4	39	12	52	18	5	102	5	3
6	52	22	53	23	11	103	23	16
7	19	2	54	113	32	104	38	25
8	28	0	55	63	22	105	31	26
11	70	23	56	84	18	106	43	16
12	47	10	57	12	3	107	50	12
13	34	16	58	12	3	108	2	1
14	14	1	59	277	113	109	8	3
15	90	30	60	78	3	110	39	30
16	25	10	62	77	14	112	68	13
17	11	3	66	39	18	113	6	0
18	60	34	67	28	7	114	8	3
19	45	25	70	66	20	115	22	7
20	18	3	72	12	0	116	184	0
21	14	8	73	6	0	117	20	8
22	10	5	74	68	27	118	33	15
23	7	3	75	47	11			
24	13	0	76	68	36			
27	71	13	77	61	28			
28	17	7	78	71	26			
29	24	4	79	39	32			

Bus	Pload	Qload	Bus	Pload	Qload
32	59	23	82	54	27
33	23	9	83	20	10
34	59	26	84	11	7
35	33	9	85	24	15
36	31	17	86	21	10
39	27	11	88	48	10
40	66	23	90	163	42
41	37	10	91	10	0
42	96	23	92	65	10
43	18	7	93	12	7
44	16	8	94	30	16
45	53	22	95	42	31
46	28	10	96	38	15
47	34	0	97	15	9
48	20	11	98	34	8

Shunt Data

Bus	G(pu)	B(pu)
5	0	-0.4
34	0	0.14
37	0	-0.25
44	0	0.1
45	0	0.1
46	0	0.1
48	0	0.15
74	0	1.1
79	0	0.2
82	0	0.2
83	0	0.1
105	0	0.2
107	0	0.06
110	0	0.06

APPENDIX D

MODIFIED 118 BUS SYSTEM DATA WITH 30% WIND PENETRATION

Bus data

Bus	Type	V (p.u.)	V(deg.)	Bus	Type	V (p.u.)	V(deg.)
1	2	0.9561	-17.78	35	1	0.9806	-17.67
2	1	0.9587	-17.01	36	2	0.98	-17.67
3	1	0.9666	-16.85	37	1	0.9917	-16.78
4	2	1.01	-13.28	38	1	0.9612	-11.59
5	1	1.0086	-12.77	39	1	0.9703	-20.18
6	2	0.99	-15.37	40	2	0.97	-21.28
7	1	0.9814	-15.71	41	1	0.9668	-21.74
8	2	1.015	-7.76	42	2	0.985	-20.18
9	1	1.0049	-0.08	43	1	0.9784	-17.35
10	2	0.9763	8.55	44	1	0.9851	-14.95
11	1	0.9756	-15.52	45	1	0.9867	-13.15
12	1	0.9691	-15.87	46	2	1.005	-10.37
212	1	1.0166	-13.55	47	1	1.0124	-8.09
312	2	1.0702	-11.46	48	1	1.0206	-8.92
13	1	0.9608	-16.97	49	2	1.025	-7.92
14	1	0.9681	-16.71	50	1	1.0208	-10.28
15	2	0.97	-17.3	51	1	1.0145	-13.23
16	1	0.9692	-16.32	52	1	1.013	-14.26
17	1	0.9943	-14.77	53	1	1.025	-15.44
18	2	0.973	-17	54	2	1.049	-14.87
19	2	0.9631	-17.49	55	2	1.032	-14.92
20	1	0.956	-16.65	56	2	1.035	-14.79
21	1	0.9554	-15.09	57	1	1.0259	-13.28
22	1	0.965	-12.55	58	1	1.0211	-14.17
23	1	0.9927	-7.63	59	1	0.9655	-9.33
24	2	0.992	-7.89	259	1	0.9978	-5.01
25	2	1.027	-0.37	359	2	1.04	-1.01
26	2	1.015	1.38	60	1	0.9642	-5.32
27	2	0.968	-13.37	61	1	0.9642	-4.35
28	1	0.9616	-15.07	261	1	0.9744	0.21
29	1	0.9632	-16.03	361	2	0.995	4.64
30	1	0.9849	-9.7	62	2	0.9738	-5.09
31	2	0.967	-15.9	63	1	0.9505	-5.75
32	2	0.963	-13.89	64	1	0.9661	-3.88
33	1	0.9715	-17.9	65	2	1.0031	-0.75
34	2	0.9857	-17.24	66	2	1.0343	-0.99

Bus	Type	V (p.u.)	V(deg.)	Bus	Type	V (p.u.)	V(deg.)
67	1	0.9998	-3.68	99	2	1.01	-1.89
68	1	0.9971	-0.76	100	2	1.0168	-0.92
69	1	1.0017	1.8	101	1	0.9913	0.67
269	1	0.9855	16.14	102	1	0.9891	3.39
369	0	1.035	30	103	2	1.0006	-4.51
70	2	0.9967	-6.55	104	2	0.971	-7.26
71	1	0.9933	-6.87	105	2	0.966	-8.38
72	2	0.98	-7.88	106	1	0.9617	-8.63
73	2	0.991	-7	107	2	0.952	-11.42
74	2	1.0117	-8.23	108	1	0.9668	-9.57
75	1	0.9863	-6.49	109	1	0.9674	-10.02
76	2	0.9518	-7.52	110	2	0.973	-10.86
77	2	0.9726	-1.86	111	2	0.98	-9.22
78	1	0.9661	-2.12	112	2	0.975	-13.96
79	1	0.9647	-1.7	113	2	0.993	-14.81
80	1	0.9769	1.04	114	1	0.9601	-14.24
280	1	0.9802	14.51	115	1	0.96	-14.25
380	2	1.04	27.15	116	2	1.005	-1.23
81	1	0.9703	-0.02	117	1	0.9524	-17.47
82	1	0.9646	-1.41	118	1	0.9638	-7.41
83	1	0.9676	-0.28				
84	1	0.9743	2.09				
85	2	0.985	3.55				
86	1	0.9867	2.18				
87	2	1.015	2.44				
88	1	0.9874	6.7				
89	2	1.005	10.77				
90	2	0.985	4.36				
91	2	0.98	4.37				
92	2	0.99	4.91				
93	1	0.9792	1.98				
94	1	0.9781	-0.12				
95	1	0.9614	-1				
96	1	0.9648	-1.02				
97	1	0.966	-0.39				
98	1	0.9834	-1.02				

Line Data

From	To	R(p.u.)	X(p.u.)	B(p.u.)
1	2	0.0303	0.0999	0.0254
1	3	0.0129	0.0424	0.0108
2	12	0.0187	0.0616	0.0157
3	5	0.0241	0.108	0.0284
3	12	0.0484	0.16	0.0406
4	5	0.0018	0.008	0.0021
4	11	0.0209	0.0688	0.0175
5	6	0.0119	0.054	0.0143
5	11	0.0203	0.0682	0.0174
6	7	0.0046	0.0208	0.0055
7	12	0.0086	0.034	0.0087
8	9	0.0024	0.0305	1.162
8	30	0.0043	0.0504	0.514
9	10	0.0026	0.0322	1.23
11	12	0.006	0.0196	0.005
11	13	0.0223	0.0731	0.0188
12	14	0.0215	0.0707	0.0182
12	16	0.0212	0.0834	0.0214
12	117	0.0329	0.14	0.0358
13	15	0.0744	0.2444	0.0627
14	15	0.0595	0.195	0.0502
15	17	0.0132	0.0437	0.0444
15	19	0.012	0.0394	0.0101
15	33	0.038	0.1244	0.0319
16	17	0.0454	0.1801	0.0466
17	18	0.0123	0.0505	0.013
17	31	0.0474	0.1563	0.0399
17	113	0.0091	0.0301	0.0077
18	19	0.0112	0.0493	0.0114
19	20	0.0252	0.117	0.0298
19	34	0.0752	0.247	0.0632
20	21	0.0183	0.0849	0.0216
21	22	0.0209	0.097	0.0246
22	23	0.0342	0.159	0.0404
23	24	0.0135	0.0492	0.0498
23	25	0.0156	0.08	0.0864
23	32	0.0317	0.1153	0.1173
24	70	0.0022	0.4115	0.102
24	72	0.0488	0.196	0.0488
25	27	0.0318	0.163	0.1764

From	To	R(p.u.)	X(p.u.)	B(p.u.)
26	30	0.008	0.086	0.908
27	28	0.0191	0.0855	0.0216
27	32	0.0229	0.0755	0.0193
27	115	0.0164	0.0741	0.0197
28	29	0.0237	0.0943	0.0238
29	31	0.0108	0.0331	0.0083
30	38	0.0046	0.054	0.422
31	32	0.0298	0.0985	0.0251
32	113	0.0615	0.203	0.0518
32	114	0.0135	0.0612	0.0163
33	37	0.0415	0.142	0.0366
34	36	0.0087	0.0268	0.0057
34	37	0.0026	0.0094	0.0098
34	43	0.0413	0.1681	0.0423
35	36	0.0022	0.0102	0.0027
35	37	0.011	0.0497	0.0132
37	39	0.0321	0.106	0.027
37	40	0.0593	0.168	0.042
38	65	0.009	0.0986	1.046
39	40	0.0184	0.0605	0.0155
40	41	0.0145	0.0487	0.0122
40	42	0.0555	0.183	0.0466
41	42	0.041	0.135	0.0344
42	49	0.0715	0.323	0.086
42	49	0.0715	0.323	0.086
43	44	0.0608	0.2454	0.0607
44	45	0.0224	0.0901	0.0224
45	46	0.04	0.1356	0.0332
45	49	0.0684	0.186	0.0444
46	47	0.038	0.127	0.0316
46	48	0.0601	0.189	0.0472
47	49	0.0191	0.0625	0.016
47	69	0.0844	0.2778	0.0709
48	49	0.0179	0.0505	0.0126
49	50	0.0267	0.0752	0.0187
49	51	0.0486	0.137	0.0342
49	54	0.0869	0.291	0.073
49	54	0.073	0.289	0.0738
49	66	0.018	0.0919	0.0248
49	66	0.018	0.0919	0.0248

From	To	R(p.u.)	X(p.u.)	B(p.u.)
49	69	0.0985	0.324	0.0828
50	57	0.0474	0.134	0.0332
51	52	0.0203	0.0588	0.014
51	58	0.0255	0.0719	0.0179
52	53	0.0405	0.1635	0.0406
53	54	0.0263	0.122	0.031
54	55	0.0169	0.0707	0.0202
54	56	0.0027	0.0095	0.0073
54	59	0.0503	0.2293	0.0598
55	56	0.0049	0.0151	0.0037
55	59	0.0474	0.2158	0.0565
56	57	0.0343	0.0966	0.0242
56	58	0.0343	0.0966	0.0242
56	59	0.0803	0.239	0.0536
56	59	0.0825	0.251	0.0569
59	60	0.0317	0.145	0.0376
59	61	0.0328	0.15	0.0388
60	61	0.0026	0.0135	0.0146
60	62	0.0123	0.0561	0.0147
61	62	0.0082	0.0376	0.0098
62	66	0.0482	0.218	0.0578
62	67	0.0258	0.117	0.031
63	64	0.0017	0.02	0.216
64	65	0.0027	0.0302	0.38
65	68	0.0014	0.016	0.638
66	67	0.0224	0.1015	0.0268
68	81	0.0018	0.0202	0.808
68	116	0.0003	0.0041	0.164
69	70	0.03	0.127	0.122
69	75	0.0405	0.122	0.124
69	77	0.0309	0.101	0.1038
70	71	0.0088	0.0355	0.0088
70	74	0.0401	0.1323	0.0337
70	75	0.0428	0.141	0.036
71	72	0.0446	0.18	0.0444
71	73	0.0087	0.0454	0.0118
74	75	0.0123	0.0406	0.0103
75	77	0.0601	0.1999	0.0498
75	118	0.0145	0.0481	0.012
76	77	0.0444	0.148	0.0368
76	118	0.0164	0.0544	0.0136

From	To	R(p.u.)	X(p.u.)	B(p.u.)
76	118	0.0164	0.0544	0.0136
77	78	0.0038	0.0124	0.0126
77	80	0.0294	0.105	0.0228
77	80	0.017	0.0485	0.0472
77	82	0.0298	0.0853	0.0817
78	79	0.0055	0.0244	0.0065
79	80	0.0156	0.0704	0.0187
80	96	0.0356	0.182	0.0494
80	97	0.0183	0.0934	0.0254
80	98	0.0238	0.108	0.0286
80	99	0.0454	0.206	0.0546
82	83	0.0112	0.0366	0.038
82	96	0.0162	0.053	0.0544
83	84	0.0625	0.132	0.0258
83	85	0.043	0.148	0.0348
84	85	0.0302	0.0641	0.0123
85	86	0.035	0.123	0.0276
85	88	0.02	0.102	0.0276
85	89	0.0239	0.173	0.047
86	87	0.0283	0.2074	0.0445
88	89	0.0139	0.0712	0.0193
89	90	0.0518	0.188	0.0528
89	90	0.0238	0.0997	0.106
89	92	0.0393	0.1581	0.0414
89	92	0.0099	0.0505	0.0548
90	91	0.0254	0.0836	0.0214
91	92	0.0387	0.1272	0.0327
92	93	0.0258	0.0848	0.0218
92	94	0.0481	0.158	0.0406
92	100	0.0648	0.295	0.0472
92	102	0.0123	0.0559	0.0146
93	94	0.0223	0.0732	0.0188
94	95	0.0132	0.0434	0.0111
94	96	0.0269	0.0869	0.023
94	100	0.0178	0.058	0.0604
95	96	0.0171	0.0547	0.0147
96	97	0.0173	0.0885	0.024
98	100	0.0397	0.179	0.0476
99	100	0.018	0.0813	0.0216
100	101	0.0277	0.1262	0.0328

From	To	R(p.u.)	X(p.u.)	B(p.u.)
100	103	0.016	0.0525	0.0536
100	104	0.0451	0.204	0.0541
100	106	0.0605	0.229	0.062
101	102	0.0246	0.112	0.0294
103	104	0.0466	0.1584	0.0407
103	105	0.0535	0.1625	0.0408
103	110	0.0391	0.1813	0.0461
104	105	0.0099	0.0378	0.0099
105	106	0.014	0.0547	0.0143
105	107	0.053	0.183	0.0472
105	108	0.0261	0.0703	0.0184
106	107	0.053	0.183	0.0472
108	109	0.0105	0.0288	0.0076
109	110	0.0278	0.0762	0.0202
110	111	0.022	0.0755	0.02
110	112	0.0247	0.064	0.062
114	115	0.0023	0.0104	0.0028

Transformer Data

8	5	100	0	0.0267
26	25	100	0	0.0382
30	17	100	0	0.0388
38	37	100	0	0.0375
63	59	100	0	0.0386
64	61	100	0	0.0268
65	66	100	0	0.037
68	69	100	0	0.037
81	80	100	0	0.037
12	212	100	0	0.05
59	259	100	0	0.05
61	261	100	0	0.05
69	269	100	0	0.05
80	280	100	0	0.05
212	312	100	0	0.05
259	359	100	0	0.05
261	361	100	0	0.05
269	369	100	0	0.05
280	380	100	0	0.05

Generator Data

Bus	Pg(MW)	Qg(MVar)	Bus	Pg(MW)	Qg(MVar)
1	0	15	15	0	16.5
4	0	84.2	18	0	27.8
6	0	41.3	19	0	-8
8	0	167.2	24	0	-4.2
10	450	-147	25	220	-47
312	85	-35	26	314	74.6

Bus	Pg(MW)	Qg(MVar)
27	0	18.4
31	7	33.1
32	0	-10.5
34	0	-8
36	0	-0.9
40	0	27
42	0	40.9
46	19	-5.2
49	204	24.1
54	48	296.5
55	0	23
56	0	-8
359	155	-51.8
361	160	-88.5
62	0	20
65	391	196.3
66	392	-67
369	522.7	24.3
70	0	32
72	0	-14.6
73	0	-4.4
74	0	9
76	0	23
77	0	70
380	477	35.4
85	0	13.4
87	4	11
89	607	-5.9
90	0	59.3
91	0	-13.1
92	0	0.5
99	0	14

Bus	Pg(MW)	Qg(MVar)
103	40	40
104	0	5.9
105	0	-8
107	0	5.7
110	0	4.9
111	36	-1.8
112	0	41.5
113	0	9.3
116	0	204.2

Shunt Data

Bus	G(pu)	B(pu)
5	0	-0.4
34	0	0.14
37	0	-0.25
44	0	0.1
45	0	0.1
46	0	0.1
48	0	0.15
74	0	1.1
79	0	0.2
82	0	0.2
83	0	0.1
105	0	0.2
107	0	0.06
110	0	0.06

Load Data

Bus	Pload	Qload	Bus	Pload	Qload
1	51	27	43	18	7
2	20	9	44	16	8
3	39	10	45	53	22
4	39	12	46	28	10
6	52	22	47	34	0
7	19	2	48	20	11
8	28	0	49	87	30
11	70	23	50	17	4
12	47	10	51	17	8
13	34	16	52	18	5
14	14	1	53	23	11
15	90	30	54	113	32
16	25	10	55	63	22
17	11	3	56	84	18
18	60	34	57	12	3
19	45	25	58	12	3
20	18	3	59	277	113
21	14	8	60	78	3
22	10	5	62	77	14
23	7	3	66	39	18
24	13	0	67	28	7
27	71	13	70	66	20
28	17	7	72	12	0
29	24	4	73	6	0
31	43	27	74	68	27
32	59	23	75	47	11
33	23	9	76	68	36
34	59	26	77	61	28
35	33	9	78	71	26
36	31	17	79	39	32
39	27	11	80	130	26
40	66	23	82	54	27
41	37	10	83	20	10
42	96	23	84	11	7

Bus	Pload	Qload
85	24	15
86	21	10
88	48	10
90	163	42
91	10	0
92	65	10
93	12	7
94	30	16
95	42	31
96	38	15
97	15	9
98	34	8
99	42	0
100	37	18
101	22	15
102	5	3
103	23	16
104	38	25
105	31	26
106	43	16
107	50	12
108	2	1
109	8	3
110	39	30
112	68	13
113	6	0
114	8	3
115	22	7
116	184	0
117	20	8
118	33	15